



universität
wien

DIPLOMARBEIT

Titel der Diplomarbeit

**The cytoplasmic cell-fate regulator MEX-5 is required for the
establishment of cortical polarity
in the *C. elegans* one-cell embryo**

angestrebter akademischer Grad

Magistra der Naturwissenschaften (Mag. rer.nat.)

Verfasserin

Silke Reiter

Matrikel-Nummer:

0304100

Studienrichtung:

Molekulare Biologie

Betreuerin:

Carrie Cowan Ph.D.

Wien, am

16. November 2009

Acknowledgements

I would particularly like to thank Carrie for giving me the chance to develop my scientific skills, for her support and advice in any situation. I also want to thank the whole group for moments of laughter and inspiring discussions.

Besonders möchte ich meiner Mutter danken, die mich durch alle Höhen und Tiefen meines Studiums begleitet hat. Von klein auf hat sie mir verdeutlicht, dass Bildung eine Chance ist sich ein selbstständiges, unabhängiges Leben aufzubauen.

Meinem Vater danke ich für seine finanzielle Unterstützung und der Möglichkeit meinen eigenen Weg zu finden und meinen Freunden, die mir gezeigt haben welche Perspektiven das Leben bietet. Ich danke ihnen für ihre aufmunternden, unterstützenden Worte und vor allem für ihre bedingungslose Freundschaft.

Table of contents

1 Abstract	1
2 Introduction	3
2.1 Cell polarity	3
2.2 C. elegans one-cell embryos as a model to understand cell polarity	5
2.3 Polarity establishment in C. elegans one-cell embryos	7
2.3.1 <i>Breaking the symmetry: Centrosome</i>	7
2.3.2 <i>Contractile polarity: Acto-myosin meshwork</i>	8
2.3.3 <i>PAR protein polarity</i>	9
2.3.4 <i>Cytoplasmic polarization: Cell fate determinants</i>	10
2.3.5 <i>Spindle alignment along the axis of cell polarity</i>	11
2.4 The cell fate regulators: MEX-5/-6	12
2.4.1 <i>MEX-5/-6 and the germline proteins</i>	12
2.4.2 <i>MEX-5/-6 structure and associated potential RNA binding function</i>	15
2.5 Aim of the project	16
3 Material & Methods	17
3.1 Worm Culture	17
3.1.1 <i>Worm strains</i>	17
3.1.2 <i>Worm maintenance</i>	17
3.1.3 <i>RNAi feeding</i>	18
3.1.4 <i>Worm lysis</i>	18
3.2 Microscopy	19
3.2.1 <i>Embryo preparation</i>	19
3.2.2 <i>Time-lapse microscopy</i>	19
3.3 DNA methods	20
3.3.1 <i>Primers</i>	20
3.3.2 <i>Plasmid</i>	20
3.3.3 <i>Polymerase chain reaction (PCR)</i>	21
3.3.4 <i>Agarose gel electrophoresis</i>	21
3.3.5 <i>Restriction reactions</i>	22

3.3.6	<i>DNA extraction from agarose gel</i>	22
3.3.7	<i>Ligation of DNA molecules</i>	22
3.3.8	<i>Transformation (electroporation)</i>	22
3.3.9	<i>Plasmid DNA purification</i>	23
3.4	Protein methods	23
3.4.1	<i>SDS- Polyacrylamide gel electrophoresis</i>	23
3.4.2	<i>Western blot</i>	24
3.4.3	<i>Detection of proteins by antibodies</i>	24
4	Results	26
4.1	MEX-5 and MEX-6 depleted embryos reveal distinguishable phenotypes	26
4.2	Localization dynamics of GFP::MEX-5	29
4.3	MEX-5 depleted embryos fail to extend the cortical PAR-2 domain	31
4.4	MEX-5 depletion affects the early phase of polarity establishment	34
4.5	Cortical contractility of mex-5(RNAi) embryos is comparable to wild type	37
4.6	Microtubule organization is not affected by MEX-5 depletion	41
5	Discussion	44
6	References	47
7	Appendix	49
7.1	Abbreviations	49
7.2	Curriculum vitae	50

1 Abstract

Polarization of the *Caenorhabditis elegans* one-cell embryo dictates asymmetric cell division into a larger and smaller blastomere, each with different fate. The sperm-supplied centrosomes provide the symmetry-breaking cue to establish an axis of polarity in the embryo. The polarizing signal is transduced into the establishment of anterior and posterior cortical domains, defining PAR protein localization. Subsequent signaling determines the plane of cell division and the segregation of cell fate determinants. MEX-5 is a cytoplasmic regulator of cell fate in *C. elegans*. MEX-5 is thought to act downstream of PAR polarity to restrict maternally supplied germline proteins to the germline (P) lineage. However recent reports (Cuenca, Schetter et al. 2003) suggest that MEX-5 may have an earlier role in polarity establishment. To investigate the role of MEX-5 in polarity establishment, I was using quantitative time-lapse microscopy to analyze MEX-5 depleted one-cell embryos. Depletion of MEX-5 results in a failure to establish PAR polarity at the onset of the first cell cycle. Loss of MEX-5 does not affect overall acto-myosin contractility or centrosome maturation. However, MEX-5 affects the centrosome-cortex proximity, indicating MEX-5's role in the early event of polarity establishment.

Zusammenfassung

Nematoda Embryonen im Einzellstadium der Klasse *Caenorhabditis elegans* entwickeln während des Zellzyklus Polarität. Diese Polarität ist verantwortlich für die asymmetrische Zellteilung des einzelligen Embryos und der Bildung verschieden großer Blastomeren mit unterschiedlicher Determination. Zentrosomen, welche vom Spermium zur Verfügung gestellt werden, erzeugen ein Symmetrie brechendes Ereignis das die Bildung einer polarisierten Achse im Embryo hervorruft. Das polarisierende Signal wird für die Erstellung einer anterior und posterior corticalen Domäne und der nachfolgenden Rekrutierung von PAR Proteinen an diese Domänen benötigt. Darauf folgende Signale bestimmen die Ebene der Zellteilung und die Segregation von Determinanten. MEX-5 beeinflusst die Distribution von cytoplasmatisch lokalisierten Determinanten in *C. elegans*. Bislang wurde MEX-5 als Übermittler der PAR Polarität und als verantwortlich für die Restriktion von Keimbahn Proteinen zur Keimbahn (P) Zelllinie beschrieben. Allerdings weisen aktuelle Berichte (Cuenca, Schetter et al. 2003) auf eine frühere Rolle von MEX-5 in der Entwicklung der Zellpolarität hin. Mit Hilfe von quantitativer Zeitraffer-Mikroskopie habe ich die Auswirkung der MEX-5 Inaktivierung während der Entwicklung der Zellpolarität analysiert. Der Abbau von MEX-5 führt zu einem Defekt in der Festlegung der Polarität am Beginn des Zellzyklus. Die Actin-Myosin Kontraktilität und die Zentrosom Assemblierung werden nicht durch den Verlust von MEX-5 beeinflusst, jedoch weist eine abweichende Zentrosom-Cortex-Nähe darauf hin, dass MEX-5 für die frühe Festlegung der Polarität notwendig ist.

2 Introduction

2.1 Cell polarity

Cell polarity reflects a crucial and complex mechanism for the establishment and maintenance of functionally specialized domains within the cell. The diverse protein composition and spatial arrangement of these domains facilitate a great variety of cellular processes, like directional cell migration, localized membrane growth and protein degradation (Drubin and Nelson 1996).

For example, neurons have a great variety in shape and length, which help the cell execute its two essential functions, transmitting signals and receiving the signals from neighbor cells. A long protrusion, the axon, is specialized to transmit signals and short, branched protrusions called dendrites are specialized to receive the signals. Establishing of neuronal polarity implicates the use of actin regulating proteins to initiate cell shape changes and microtubule modulators to generate or maintain differences in morphology (Rolls and Doe 2003). Epithelial cells use a polarizing signal to form cytoskeletal and signaling networks to partially reorganize the cell, whereas *D. melanogaster* neuroblasts and the *C. elegans* one-cell embryo establish polarity to give rise to cells with different fates.

The process of cell differentiation, in which cells become structurally and functionally different from each other, depends on two phases: polarity establishment and polarity maintenance, resulting in asymmetric cell division.

An initial cue provides the information to establish structural and molecular asymmetries at the cell surface. The further interpretation of the signal from this cue generates new membrane domains and reorganization of the cell. Polarity is maintained by feedback regulation at each stage, which coordinates the proper ordering of these events (Drubin and Nelson 1996; Cuenca, Schetter et al. 2003).

Information guiding asymmetric cell division can be either of internal or external origin. According to the type of information, divisions have been classified into “intrinsic” or “extrinsic”. A division is intrinsic if cell fate determinants are unequally distributed and segregated to one daughter cell. Extrinsic asymmetric cell division is the acquirement of distinct fates of initially equivalent daughter cells by post-mitotic signals (Abrash and Bergmann 2009).

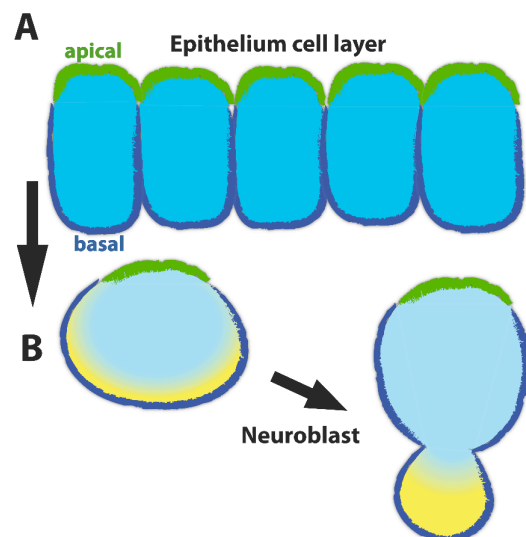
An example for intrinsic asymmetric cell division is the differentiation of *Drosophila* neuroblasts (Figure 1). With each cell division they give rise to a large neuroblast cell and a smaller cell that continues dividing to neurons. The neuroblasts delaminate from the monolayered epithelium and polarization along the apical-basal axis facilitates asymmetric cell division. Proteins required for apical-basolateral polarity are maintained during neuroblast delamination and recruit polarity determinants to the cortex. These polarity proteins restrict cytoplasmic cell fate determinants to the opposite site of the cell and orient the mitotic spindle by attracting one of the spindle poles to facilitate asymmetric cell division (Knoblich 2008).

An example for extrinsic asymmetric cell division is the differentiation of ovarian germline stem cells to oocyte and nurse cells in *Drosophila melanogaster* (Figure 2). The ovarian germline stem cells are in close contact with the stem cell niche from which they receive a signal essential for self-renewal.

Figure 1. Intrinsic asymmetric cell division

[A] Epithelium cell layer with apical (green) and basal (dark blue) domain

[B] *Drosophila* neuroblasts, an example for intrinsic asymmetric cell division, delaminate from the epithelium cell layer and recruit polarity determinants to the former apical domain to restrict cell-fate determinants (yellow) to the opposite site of the cell. The cell divides into a larger neuroblast and a smaller neuron precursor.

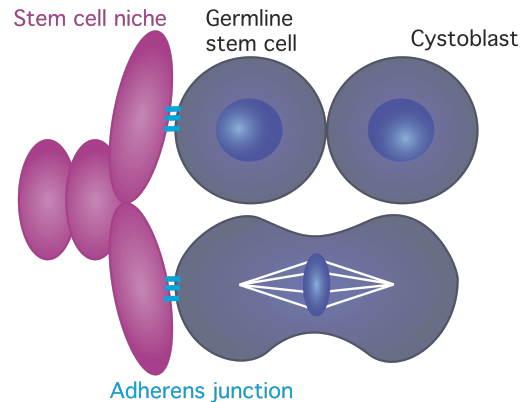


The mitotic spindle orients perpendicular to the surface of the stem cell niche in dividing ovarian germline stem cells. Therefore, one daughter cell (cystoblast) is displaced from the stem cell niche and the self-renewal signal is no longer transmitted to the cell. Differentiation is up regulated in the cystoblast and the oocyte and the nurse cells are finally formed (Neumueller and Knoblich 2009).

The execution of asymmetric cell division requires the coordination of several distinct processes. A mechanism that determines the plane of cell division and therefore the correct positioning of mitotic spindle must be coordinated with the segregation of cell fate determinants in a way that unequal daughter cells are generated (Abrash and Bergmann 2009).

Figure 2. Extrinsic asymmetric cell division

Germline stem cells (grey) are in contact with the stem cell niche (pink) through adherens junctions (light blue). After cell division the daughter cell is no longer in contact with the niche and becomes the cystoblast.



2.2 *C. elegans* one-cell embryos as a model to understand cell polarity

It all began with Sydney Brenner, who started in 1967 to develop the genetics of the model organism: *Caenorhabditis elegans* (Figure 3). He discovered the big advantages of the nematode, namely that it is small, rapidly growing, and easily handled in laboratory (Brenner 2009).

C. elegans increased its popularity as model system in the year of 1998, where it became the first multicellular organism for which a complete genome sequence was obtained (Hodgkin 2005).

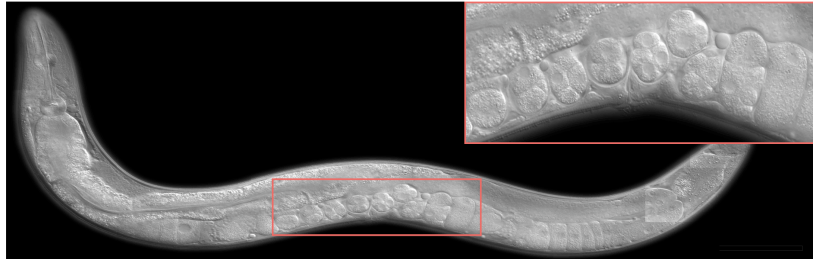


Figure 3. Adult *Caenorhabditis elegans*

The higher magnification shows the development of the one-cell embryo (rightmost embryo) to a multi-cellular embryo (to the left) within the nematode.

From Ian D. Chin-Sang, <http://www.nematode.net> © Washington University School of Medicine and the Genome Sequencing Center

The *C. elegans* one-cell embryo (Figure 4A) is a favored model system to study cell polarity. The first cell division is asymmetric and divides the cell into the larger anterior blastomere AB and the smaller posterior blastomere P1 (Figure 4B), which is the precursor of the germline lineage (Goenczy and Rose 2005). Followed by four asymmetric cell divisions the embryo produces six founder cells: AB, MS, E, C (Figure 4D), D and P4, each of which produces a specific subset of cell types. These early cleavages define the three principle axes of the body plan.

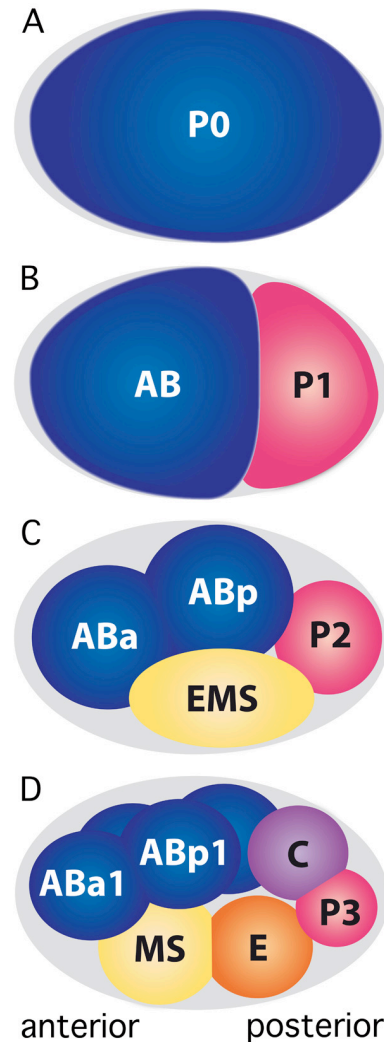


Figure 4. Asymmetric cell division in the early embryo

(anterior is to the left, posterior to the right)

The generation of founder cells is shown in the early embryo, from the one-cell stage to the eight-cell stage [A-D]. The germ-line precursors (P lineage) are shown in pink [B-D].

The sperm derived centrosome provides the symmetry-breaking cue for the embryo to establish anterior-posterior polarity. The dorso-ventral axis appears between the transition of two-cell and four-cell stage (Figure 3 B-C), with EMS defining the ventral side of the embryo. The left-right axis is detectable between the four-cell and six-cell stage, the location of AB defines the left side of the embryo (Goenczy and Rose 2005).

2.3 Polarity establishment in *C. elegans* one-cell embryos

2.3.1 Breaking the symmetry: Centrosome

The anterior-posterior axis of the *C. elegans* one-cell embryo is determined shortly after fertilization. Initiation of polarity requires a symmetry-breaking event, which induces contractile polarity of the cortex and the establishment of cortical domains (Figure 5).

Laser ablation studies of the sperm supplied centrosome, prior to and after polarity establishment, demonstrated a direct contribution of the centrosome in polarity initiation but not in polarity maintenance.

Furthermore, the movement of the centrosome to the cortex is temporally and spatially correlated with the posterior domain formation (Cuenca, Schetter et al. 2003; Cowan and Hyman 2004b).

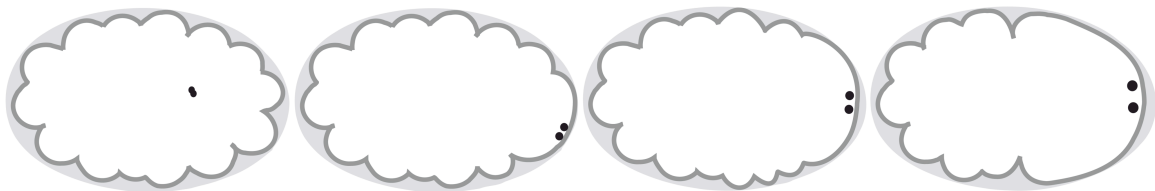


Figure 5. Centrosome migration during polarity establishment

C. elegans embryos from entry into the first cell cycle (left), to the completion of polarity establishment (right). Dark gray outline of the embryo indicates the contractile polarity. Centrosome (black dots) duplicates and the pair of centrosome migrates toward the posterior cortex (to the right).

2.3.2 Contractile polarity:

Acto-myosin meshwork

The establishment of anterior-posterior polarity in the *C. elegans* one-cell embryo depends on the formation of cortical domains. The contractile polarity represents one type of cortical domain, defined by different contractile activity of the anterior and posterior cortex.

After completion of the second meiotic division, the embryo surface starts ruffling, visible as a series of contractions resulting in numerous invaginations of the cortex (Figure 6). The driving force is a meshwork built of actin filaments, myosin filaments and additional cross-linking proteins. The myosin filaments, composed of type II myosin, cross-link actin filaments to build up the acto-myosin meshwork. The acto-myosin meshwork causes ruffling of the cell surface that results in both reorganization and remodeling of the cortex.

Before polarity is initiated, the whole embryo surface undergoes ruffling. A polarizing signal provided at the posterior cortex causes the initiation of cortical smoothing in the area around the sperm supplied centrosome.

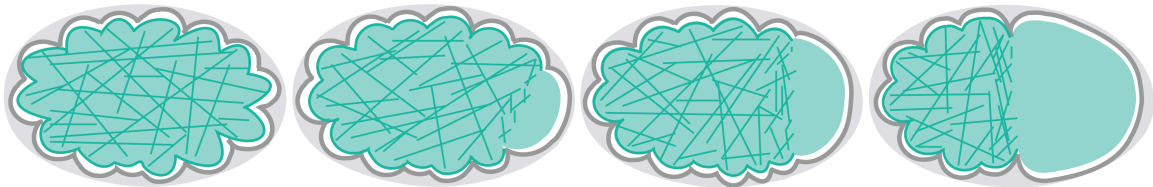


Figure 6. Acto-myosin meshwork in the one-cell embryo

C. elegans embryos from entry into the first cell cycle (left), to the completion of polarity establishment (right). The acto-myosin meshwork shown in green is indicated from a surface view of the embryo cortex. The smoothing domain at the posterior (to the right) expands toward the embryo's anterior (left).

The extension of the smooth domain to the midline of the embryo results in a deeper and more stable ingression at the leading edge of the domain (pseudo-cleavage furrow), whereas the anterior domain continues to ruffle (Cowan and Hyman 2004b).

Acto-myosin contractility depends on the activity of the RhoGTPase, which is controlled by two factors (Jenkins, Saam et al. 2006; Motegei and Sugimoto 2006; Schonegg and Hyman 2006).

The CYK-4 Rho GAP (GTPase activating protein) inhibits Rho and the ECT-2 GEF (Guanidine nucleotide exchange factor) activates Rho activity and thus activate contractility (Glotzer 2005). A possible model for the establishment of contractile polarity is the local down-regulation of Rho activity by Rho GAP CYK-4 and the exclusion of the activating factor RhoGEF ECT-2 from the posterior domain (Cowan and Hyman 2007).

2.3.3 PAR protein polarity

Another type of cortical domain in the *C. elegans* one-cell embryo consists of PAR (partitioning defective protein) proteins. PAR proteins are highly conserved polarity regulators, which show asymmetric localization in *C. elegans* along the anterior-posterior axis.

A complex composed of the scaffold proteins PAR-3, PAR-6 and the atypical protein kinase C (aPKC) defines the anterior domain, whereas the serine threonine kinase PAR-1 and the ring domain protein PAR-2 define the posterior domain (Figure 7) (Cuenca, Schetter et al. 2003).

The formation of these domains is driven by the asymmetric contraction of the cortical acto-myosin meshwork, which causes cortical flows directed away from the sperm supplied centrosome, towards the future anterior pole. The complex consisting of PAR-3/PAR-6/aPKC is transported through cortical flow to the anterior pole, which corresponds precisely with the contractile domain (Cheeks, Canman et al. 2004; Munro, Nance et al. 2004).

Studies in *C. elegans* and other model organisms suggest that the anterior PAR domain may antagonize the posterior PAR proteins, thus removal of PAR-3/PAR-6/aPKC to the anterior presumably allows PAR-1 and PAR-2 level to rise at the posterior (Cowan and Hyman 2004b; Munro 2006).

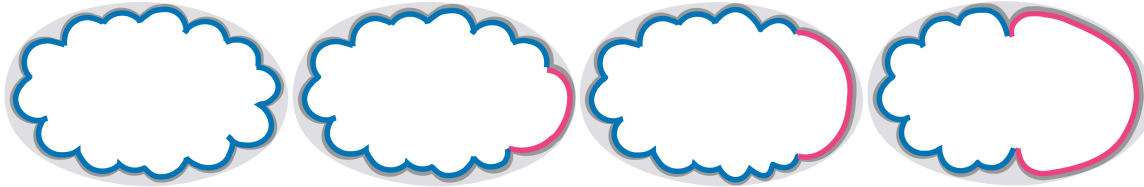


Figure 7. Establishment of PAR protein polarity

C. elegans embryos from entry into the first cell cycle (left), to the completion of polarity establishment (right). PAR-3, PAR-6 and aPKC localization is shown in blue (anterior); PAR-1 and PAR-2 localization is shown in red (posterior).

2.3.4 Cytoplasmic polarization: Cell fate determinants

Polarity at the cortex is transmitted to the cytoplasm by downstream signaling of the PAR proteins and by the generation of cytoplasmic flow toward the posterior pole (Cheeks, Canman et al. 2004). Cytoplasmic polarization is required for the unequal distribution of cell fate determinants and other determinants, which act as transducers of cortical polarity to downstream effectors necessary for asymmetric cell division (Hird and White 1993).

The cell fate determinant PIE-1 (Mello, Schubert et al. 1996) and the mediators of cell fate POS-1 (Tabara, Hill et al. 1999) and MEX-1 (Mello, Draper et al. 1992; Guedes and Priess 1997) are required for the maintenance of the P-lineage fate and segregate during each asymmetric division preferentially to the germline blastomere (Figure 7A-C).

Further regulators of cell fate are the cytoplasmic proteins MEX-5/-6 (see section 2.4), which restrict germline proteins to the posterior pole of the one-cell embryo (Schubert, Lin et al. 2000).

PIE-1/POS-1 and MEX-1 are zinc finger proteins and show association with P-granules, RNA rich cytoplasmic “germ granules” (DeRenzo, Reese et al. 2003). Imaging of fluorescently labeled P-granules in the one-cell embryo reveals the movement to the posterior pole by flows. The knock down of a cortically enriched myosin II motor, *nmy-2*, suggests that cortical and cytoplasmic flows deliver P-granules to the posterior pole of the embryo (Cheeks, Canman et al. 2004).

2.3.5 Spindle alignment along the axis of cell polarity

The correct segregation of cell fate determinants to the daughter cells during asymmetric cell division requires spindle positioning along the axis of cell polarity. Cortical polarity, determined by the PAR proteins, is transduced to the spindle by effector proteins to ensure proper spindle positioning (Cheng, Kirby et al. 1995; Goenczy and Rose 2005). Those effectors generate unequal pulling forces at the cortex to move the posterior spindle pole toward the posterior of the embryo, leading to asymmetric cell division.

Spindle positioning follows basically two processes: alignment of the centrosomes along the anterior-posterior axis and asymmetric displacement of the spindle towards the posterior pole. After polarity is established, the female pronucleus migrates toward the male pronucleus in the embryo posterior (Figure 8A). The pronuclei move together with the associated centrosomes toward the center of the embryo and the whole complex rotates by 90° so that the centrosomes are aligned with the anterior-posterior axis (Figure 8B) (Albertson 1984; Hyman and White 1987). Unequal pulling forces at the cortex acting on astral microtubules (Grill, Gönczy et al. 2001) displace the posterior spindle pole toward the embryo posterior followed by the anterior spindle pole, thus dictating unequal cleavage (Figure 8C).

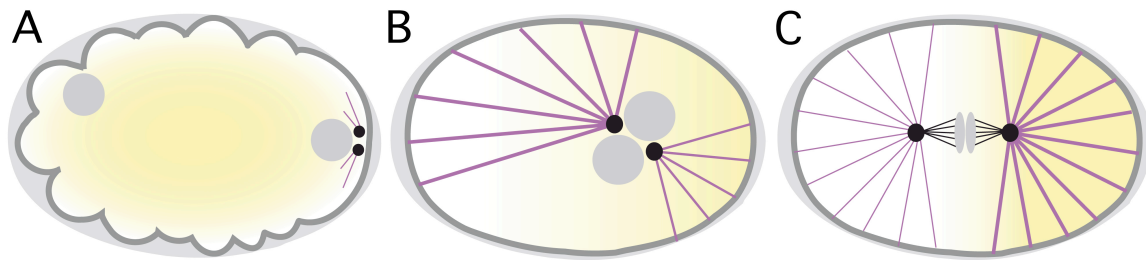


Figure 8. Segregation of cell fate determinants

[A] One-cell embryo during polarity establishment showing pronuclei as grey circles, centrosomes (black dots), microtubules (purple) and the uniform distribution of cell fate determinants in yellow. Dark grey outline of the embryo indicates contractile polarity.

[B] After pronuclei meeting: the complex consisting of pronuclei and centrosomes rotate by 90°. Different pulling forces acting on microtubules are indicated by different strength of the lines.

[C] The spindle poles are aligned along the anterior (left) -posterior (right) axis. Different pulling forces move the posterior spindle pole toward the posterior, thus dictating asymmetric cell division. Cell fate determinants are unequally distributed to one half of the embryo.

2.4 The cell fate regulators: MEX-5/-6

Two zinc-finger proteins, MEX-5 and MEX-6 were initially shown to transmit cortical PAR polarity downstream to germline proteins (Schubert, Lin et al. 2000). However, further investigation revealed, that MEX-5 affects PAR polarity (Cuenca, Schetter et al. 2003) and therefore leads to the suggestion that MEX-5 may have a role in polarity establishment in the *C. elegans* one-cell embryo.

2.4.1 MEX-5/-6 and the germline proteins

MEX-5 has been originally identified in a genetic screen for mutants with muscle excess (MEX) phenotype, due to the mis-expression of the transcription factor SKN-1. The posterior protein SKN-1 is required for the development of muscles

in the pharynx, mis-expression in the anterior blastomere results in abnormally large numbers of muscles.

One mutation was localized to the predicted gene W02A2.7 on chromosome V, which has been named *mex-5*. Furthermore, the gene sequence AH6.5 encodes a protein that is about 70 % identical and 85 % similar to MEX-5 in amino acid sequence, hence named MEX-6.

Mutant analysis showed that embryos produced from homozygous *mex-5* adults die without hatching, whereas *mex-6* embryos were viable and grew into fertile, normal adults. Thus *mex-6* appears to be a nonessential gene.

Embryos from *mex-5; mex-6* adults exhibit a uniform distribution of posteriorly localized germline proteins PIE-1, MEX-1 and POS-1. Additionally, in wild type embryos, the cytoplasmic P-granules asymmetrically segregate to germline blastomeres, whereas in *mex-5; mex-6* embryos the P-granules were present in all blastomeres (Schubert, Lin et al. 2000).

MEX-5/-6 and PIE-1 are initially uniformly distributed throughout the cytoplasm. As the cell cycle proceeds, MEX-5/-6 and PIE-1 start to exhibit opposite distributions. After the appearance of the smooth cortical domain at the posterior, MEX-5/-6 begins to accumulate in the anterior cytoplasm and PIE-1 levels increase in the posterior simultaneously. Maximal asymmetry is reached by pseudocleavage. Finally, cell division segregates PIE-1 to the germline blastomere and MEX-5/-6 are predominantly restricted to the anterior blastomere with somatic fate (Cuenca, Schetter et al. 2003).

Thus, mutant analysis and investigation of protein localization suggest that MEX-5/-6 are required to restrict germline proteins to the germline (P) lineage. On the contrary, *par-1* mutant embryos exhibit symmetric distribution of MEX-5 (Schubert, Lin et al. 2000). These results indicate that PAR-1 is necessary to restrict MEX-5 to the anterior of the embryo (Figure 9A) (Kemphues 2000).

In the early embryo, almost all of the mRNA's encoding both, anterior and posterior localized proteins is distributed uniformly throughout the embryo (Evans, Crittenden et al. 1994; Seydoux and Fire 1994; Guedes and Priess 1997; Schubert, Lin et al. 2000). How do protein asymmetries arise? Asymmetries must result either from protein movement, differences in mRNA translation or diverse protein stability.

For example, turnover of PIE-1 level in the anterior blastomere is mediated by degradation, which depends on the specific targeting of PIE-1's zinc finger domain by ZIF-1, a protein identified in a yeast-two-hybrid assay. ZIF-1 showed interaction with PIE-1, POS-1, MEX-1 and MEX-5, all of them contain a tandem zinc

finger domain, that when mutated interaction was blocked. Further findings suggest that ZIF-1 acts as a substrate-recruitment subunit for an E3 ubiquitin ligase. Furthermore MEX-5/-6 are required to activate ZIF-1 dependent degradation in somatic blastomeres. Thus, MEX-5/-6 specifically facilitate degradation of PIE-1, POS-1 and MEX-1 in somatic blastomeres, resulting in asymmetric localization to the germline blastomere (Figure 9B) (DeRenzo, Reese et al. 2003).

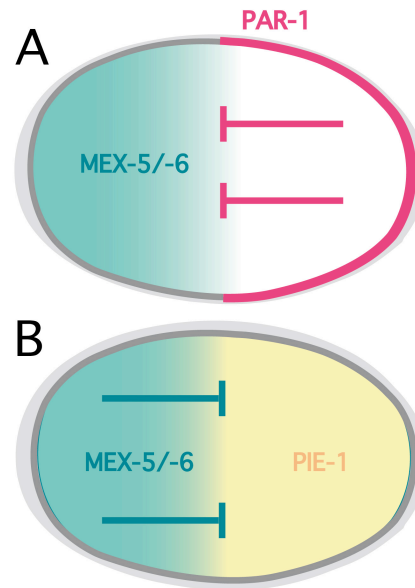


Figure 9. Repression model

[A] PAR-1 (red) restricts MEX-5/-6 (green) to the anterior (to the left) pole of the embryo.

[B] Subsequently MEX-5/-6 restrict germline proteins, here represented by PIE-1 (yellow), to the embryo's posterior.

2.4.2 MEX-5/-6 structure and associated potential RNA binding function

MEX-5 and MEX-6 are CCCH-type tandem zinc finger proteins (Schubert, Lin et al. 2000), a similar motif was first described in the vertebrate protein tristetrin (TTP) (Varnum, Ma et al. 1991).

TTP specifically recognizes nonameric UUAUUUAUU sequences in the 3' untranslated region (UTR) of mRNA to regulate stability and translation efficiency. A proposed mechanism for MEX-5/-6 regulatory function in the one-cell embryo is derived from TTP's RNA binding ability. RNA binding activity may contribute to maternal RNA regulation and, as a consequence, direct patterning the anterior-posterior axis. Investigation of MEX-5's RNA binding function reveals that high affinity binding does not require UAUU repeats in the 3' UTR. However, further results demonstrate that MEX-5 binds with high affinity to a tract of 6-8 uridines within an 8-nucleotide window. However, binding to polyuridine tracts does not provide enough specificity to select mRNAs for regulation because of their abundance in 91 % of *C. elegans* 3' UTR sequences.

In contrast, TPP binds selectively and with high affinity to UAUU repeat sequences, therefore TPP regulates specifically the translation of mRNA in vertebrates.

Each zinc finger contains a highly conserved region that directs specificity. Consequently, differences between TPP and MEX-5 in the amino acid sequence could be responsible for the diverse binding specificity. The first zinc finger domain of the predicted RNA binding pocket in MEX-5 has an arginine residue instead of glutamate and lysine in the second zinc finger, suggesting that glutamate residues encode selectivity for UUAUUUAUU RNA and basic residues facilitate binding to uridine-rich RNA sequences.

MEX-5 alone is not able to provide enough specificity to drive regulation of maternal transcripts, thus an additional RNA binding protein that interacts with MEX-5 may provide specificity (Pagano, Farley et al. 2007). For example, in *Drosophila* embryos the maternal RNA-binding proteins Pumilio and Nanos act together to regulate translation of specific mRNA in germline progenitors (Asaoka-Taguchi, Yamada et al. 1999).

Recent reports suggest that PLK-1/2 binding regulates MEX-5/-6 function to restrict germline proteins to the P-lineage. PLK-1 and PLK-2 are known key regulators in cell division, beside that they might play a role in regulating MEX-5/-6 function. The polo box domain of PLK-1 and PLK-2 show physical interaction with the phosphorylated T₁₈₆ site of MEX-5. Subsequent phosphorylation of MEX-5 by PLK-1/PLK-2 might change binding affinities toward mRNA targets or interacting proteins (Nishi, Rogers et al. 2008).

2.5 Aim of the project

The cytoplasmic cell fate regulators MEX-5/-6 act downstream of PAR polarity to restrict germ line proteins to the germ line lineage. Moreover, more recent investigations suggest that MEX-5 may have a role in polarity establishment (Cuenca, Schetter et al. 2003).

The aim of the project is to further investigate the role of MEX-5 and MEX-6 in polarity establishment. To achieve that, *mex-5* and *mex-6* depleted embryos were quantitatively and phenotypically analyzed by time-lapse microscopy. RNAi depletion was applied to embryos carrying fluorescently tagged markers to assess cortical domain formation, centrosomes and cortical ruffling.

3 Material & Methods

3.1 Worm Culture

3.1.1 Worm strains

Strain	Description	Genotype
JH1448*	GFP::MEX-5	axEx1125[pKR2.04+pRF4+mex-5::GFP]
N2	N2	wild type strain
TH119	GFP::PAR-2; mCH::PAR-6	GFP::PAR-2::rol-6; mCH::PAR-6::unc-119(+)
WH510	cGFP	unc-119(ed3) III, ojEx92[GCaMP; unc119(+)]
TH42	GFP::SPD-2	GFP::SPD-2::unc-119(+); unc-119(ed3)
UE21	GFP::SPD-2; GFP::NMY-2	GFP::SPD-2::unc-119(+); GFP::NMY-2::unc-119(+)
XA3501	GFP::H2B; GFP::β-tubulin	unc-119(ed3) ruls32[unc-119(+) pie-1::GFP::H2B] III; ojs1[unc-119(+) pie-1::GFP::tbb-2]

* acquired from the *Caenorhabditis* genetics center (CGC), University of Minnesota

3.1.2 Worm maintenance

Worm strains were maintained by passing them 2-3 times per week to new plates. The tip of a pasteur pipet was prepared with a piece of platinum wire to transfer worms from one petri plate to another. For maintenance, 2 or 3 worms were picked with the sterile, flattened tip of the wire. Worms were fed with the uracil auxotroph *E.coli* strain OP50 seeded on NGM plates. The nematode growth medium (NGM) restricts the growth of the *E. coli* strain.

Strains were kept regularly at 16°C. Worms determined for microscopy were put for 24 hours at 24°C to obtain the proper expression of the fluorescence protein.

3.1.3 RNAi feeding

This approach was used to knockdown gene function within the embryo. The HT115 bacterial strain was used as host for vector clones expressing dsRNA, because of the IPTG inducible polymerase and the disrupted RNase III gene. The plasmid carrying the desired gene was transformed by electroporation into HT115. A single colony was picked and inoculated into 2 ml LB +carb (carbenicillin c[25µg/ml]) +tet (tetracycline c[10µg/ml]) and incubated at 37°C for approximately 16 hours. 100 µl of the starter culture was inoculated in 5 ml LB +carb and incubated for 3 hours at 37°C. To start expression of the cloned sequence, 15 µl IPTG (3 mM) was added to the bacteria suspension and incubated for additional 30 min. 250 µl of the bacteria culture was seeded on NGM feeding plates (Ø 4 cm) containing additional IPTG. The plates were kept at room temperature for 2-3 days until the bacteria lawn was well grown and then stored at 4°C. The efficient knockdown of a desired gene required investigation of the right incubation time. L4 stage worms were put on RNAi feeding plates for 24 to 48 hours at 24°C before recording. Because of inefficient knockdown, the incubation time was increased up to 65 hours. Adult worms layed embryos on the RNAi feeding plates, which were then incubated for 65 hours at 24°C.

3.1.4 Worm lysis

Worms were lysed for protein analysis and protein detection by antibodies. Each worm strain was grown either on OP50, N2 or RNAi feeding bacteria NGM plates (8 cm). 25 worms were put into safe lock tubes prepared with 0.5 ml 0.1 M NaCl. After two washing steps with 0.1 M NaCl and centrifugation at 4,000 rpm for 3 min the supernatant was removed up to 12.5 µl. The worm containing solution was frozen in liquid N₂ and immediately thawed with additional equal volume of 2x sample buffer. The water bath sonicator was heated up to 80 °C and the tubes containing the worms were sonicated 3 times for 5 min.

Finally the lysed worms were separated from the cell material by centrifugation for 5 min at 14,000 rpm. Before loading onto SDS-PAGE gel, the extract was boiled for 5 min at 95 °C.

3.2 Microscopy

3.2.1 Embryo preparation

Two different methods were used to prepare the embryos for recording. For the “agarose patch” method the worms were dissected in 4 μ l 0.1 M NaCl +4% sucrose solution to release the embryos. The cover slip with the embryos was inverted onto a 2 % agarose patch and viewed with the selected microscope. The “hanging drop” method was used especially for recordings before polarity was established in the one-cell embryo. 15 μ l of Poly-L-Lysine (Sigma) were dried two times on a cover slip to produce a sticky surface. For dissecting the worms, 3 μ l of EGM (PVP, Inulin, NaCl, 0.25 M HEPES, penicillin/streptomycin, galactose, lactose, glutamine, pyric acid, FBS) solution were put on the sticky surface. Finally, a cover slip was put on the sticky surface and the embryos were ready for viewing.

3.2.2 Time-lapse microscopy

GFP and mCH localization dynamics were analyzed by time-lapse microscopy. Single plane images of the mid-focal plane were collected typically at 15 seconds intervals using 40x/1.2 plan-neofluar objective. Images were acquired using a Photometrics CoolSnap HQ2 camera attached to a Zeiss Axiovert 200M equipped with HBO 103W halogen lamp, GFP filter (Ex 500/25nm, Em 535/30nm) and RFP filter (Ex 472/30nm, Em 520/35nm). Image acquisition was controlled by MetaMorph software (7.1.2).

3.3 DNA methods

3.3.1 Primers

Primers for MEX-6 cloning

5' – TTC TAG ACC CAA CGT ACA CGG CAC AAA – 3'

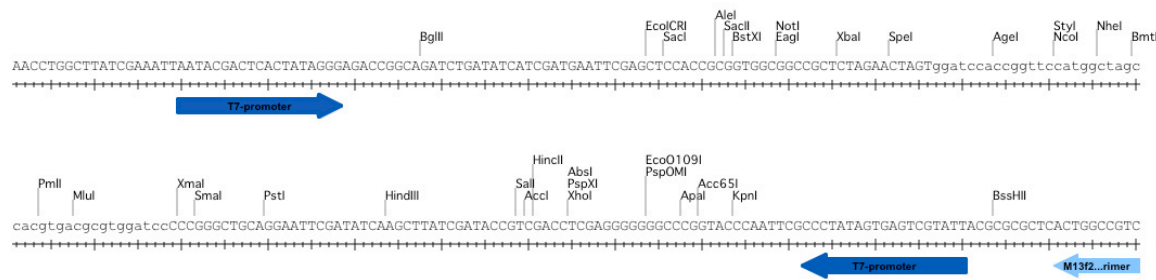
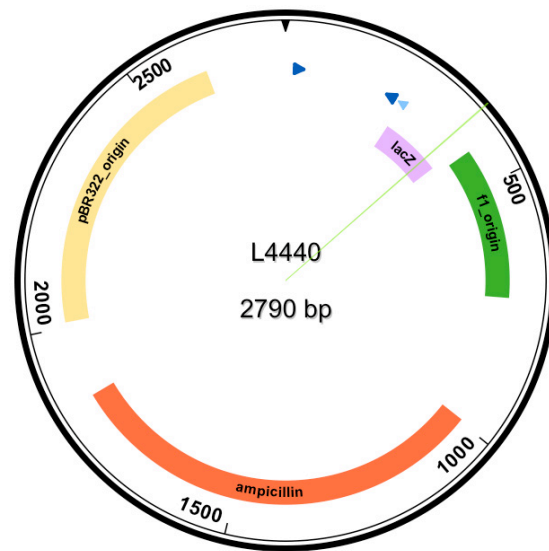
5' – AGC CAT GGA TCG TCG TTG TGA TTG TC – 3'

Primer for L4440 sequencing

5' – ACG ACG TTG TAA AAC GAC – 3'

3.3.2 Plasmid

Figure 9. Schema of L4440 plasmid
Target gene was cloned between T7 promoter (dark blue) sequences to generate expression of dsRNA in HT115 feeding bacteria. Additional schema shows the insertion site of the gene, the multiple cloning site between the T7 promoters.



3.3.3 Polymerase chain reaction (PCR)

The amplification of DNA fragments was performed on a DNAEngine Peltier Thermal Cycler (BioRad). For a reaction volume of 50 μ l approximately 10 ng DNA template, 10 pmol of each primer, 5 μ l 10x long enzyme buffer, 100 μ M dNTP and 0.5 units of long PCR enzyme mix (Fermentas) were used.

Purification of the PCR product was performed with the QIAquick PCR purification kit according to the manufacturers protocol. PCR products were eluted in 30 μ l dH₂O.

Colony PCR was performed to check clones for successfully inserted DNA fragment. After the ligation mixture was transformed into the bacteria the resulting colonies were picked and inoculated into 5 μ l dH₂O. The PCR reaction volume for each colony was 25 μ l containing 2.5 10x Taq buffer, 2.5 mM MgCl₂, 100 μ M dNTP, 0.5 μ l DMSO, 0.4 units Taq polymerase (Fermentas), 10 pmol of each primer and 1 μ l of the bacteria suspension.

3.3.4 Agarose gel electrophoresis

DNA samples were analyzed on 1% agarose gels including ethidiumbromide (1:10000) for the detection of DNA. The DNA samples were mixed with 6x Orange DNA loading dye (Fermentas) and diluted with dH₂O to an appropriate volume. The samples and 3 μ l of the express DNA ladder (#SM1553 Fermentas) were loaded on the gel. Separation was performed in TAE buffer at 120 V for 20 min. Finally, the gels were visualized with the UV-transilluminator.

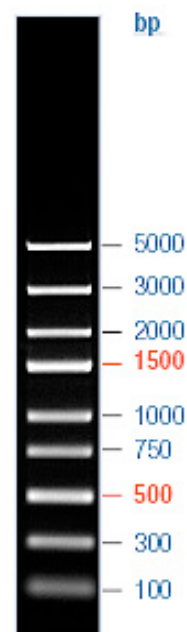


Figure 10. DNA ladder
Fermentas, #SM1553

3.3.5 Restriction reactions

30 μ l of the PCR product was digested with 1 μ l NcoI (Fermentas), 1 μ l XbaI (Fermentas) and 3.2 μ l 10x Tango buffer (Fermentas). For Plasmid (L4440) digestion approximately 10 μ g plasmid DNA, 0.5 μ l XbaI, 0.5 μ l NcoI and 1 μ l 10x Tango buffer was used. Both reactions were incubated at 37 °C for 3 hours and cleavage was monitored by agarose gel electrophoresis.

3.3.6 DNA extraction from agarose gel

After cleavage performance the samples were loaded onto a 1 % agarose gel containing 10,000x SYBR Safe DNA gel stain (Invitrogen) followed by running the gel at 200 V for 30 min. The DNA band was cut out from the agarose gel, visualized by the Safe Imager (Invitrogen). DNA extraction was performed according to the manufacturers protocol (QIAEX II QIAGEN). DNA was eluted with 20 μ l H₂O.

3.3.7 Ligation of DNA molecules

A total reaction volume of 10 μ l was used, containing 1 μ l digested plasmids, 8 μ l digested DNA fragments, 1 μ l 10x T4 ligase buffer and 1 μ l T4 ligase (Promega). The reaction was carried out overnight at 16 °C. Additional negative controls were included.

3.3.8 Transformation (electroporation)

Transformation of plasmids was performed by electroporation. 50 μ l of electro-competent DH5 α bacteria cells, stored at -80°C were thawed on ice and then mixed with 1.5 μ l ligation product.

The mixture was transferred to a pre-chilled electroporation cuvette and transformation was performed at 2.5 Amp (BioRad *E. coli* Pulser).

After the electroporation, 1 ml LB medium was immediately added to the bacteria and allowed to recover for 30 min at room temperature. Subsequently, the bacteria were plated onto LB + amp (Ampicillin) plates and incubated overnight at 37°C. Single colonies were picked and analysed by colony PCR.

3.3.9 Plasmid DNA purification

The GeneJET Plasmid Miniprep Kit (Fermentas) was used to isolate plasmid DNA from bacteria. 4 ml LB +Amp +Tet were inoculated with one bacterial colony and grown overnight at 37 °C shaking 220 rpm. Plasmid isolation was performed according to the manufacturer's protocol.

3.4 Protein methods

3.4.1 SDS- Polyacrylamide gel electrophoresis

SDS – polyacrylamide gel electrophoresis (SDS-PAGE) was used to separate proteins according to their molecular weight. Binding of the negatively charged detergent sodium dodecyl sulphate (SDS) causes unfolding and migration of the proteins toward the positive electrode.

Samples were mixed with equal volume of 2x Laemmli sample buffer (Sigma) and incubated for 5 min at 95°C.

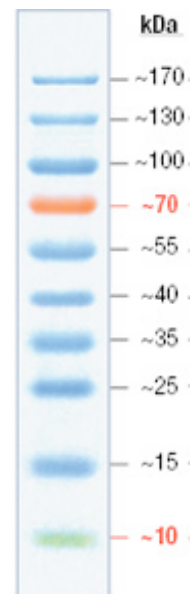


Figure 11. Prestained protein ladder
Fermentas, #SM0671

The denatured proteins were loaded on NuPAGE 4-12 % Bis-Tris gel (Invitrogen) together with 5 μ l of prestained protein ladder (#SM0671 Fermentas). Electrophoresis was carried out at 200 V for 50 min (MOPS SDS Running buffer, Invitrogen).

3.4.2 Western blot

Proteins separated by SDS-PAGE were transferred to a Protran BA85 nitrocellulose membrane (Whatman). 6 sponges, 6 Whatman papers and the nitrocellulose membrane were soaked in transfer buffer (20 % MeOH, 25 mM Tris, 190 mM glycine, 0.02 % SDS) and assembled to a blotting sandwich.

Order of blotting sandwich: **ANODE** 3 sponges – 3 Whatman papers – nitrocellulose membrane – polyacrylamide gel – 3 Whatman papers – 3 sponges **KATHODE**. The blotting sandwich was put into the chamber of the blotting apparatus (NuPAGE Invitrogen) and the inside was filled up with transfer buffer. The proteins were blotted towards the anode at 400 ampere for 2 hours. Afterwards the proteins were reversibly stained with ponceau S dye to observe protein transfer efficiency.

3.4.3 Detection of proteins by antibodies

The blot was incubated for 1 hour in PBS +0.5 % Tween-20 +10 % milk to block unspecific binding of the antibody to the nitrocellulose membrane. Subsequently, the blot was incubated from 1 to 4 hours, depending on the antibody, with 10 ml of a primary antibody dilution (1:200 dilution anti-GFP mouse monoclonal IgG_{2a}, 1:1000 dilution anti- α tubulin mouse antibody, Santa Cruz Biotechnology) at room temperature.

After one fast washing step and two washing steps for 15 min with 1x PBS +0.5 % Tween-20, the blot was incubated for 1 hour with 10 ml of the secondary antibody dilution (1:2000 dilution anti-mouse HRP conjugate).

Followed by two washing steps for 15 min with PBS +0.5 % Tween and two final washing steps for 10 min with PBS. The ECL detection reagents I and II (Amersham) were equally mixed and put onto the membrane for 1 min. The detergents elicit a peroxidase-catalyzed oxidation of luminol, which enhances chemiluminescence. The resulting light was detected on Hyperfilm ECL (Amersham) in 5 to 30 sec.

4 Results

4.1 MEX-5 and MEX-6 depleted embryos reveal distinguishable phenotypes

I used the technique of double stranded RNA mediated depletion to examine potential functions of MEX-5 and MEX-6 during polarity establishment. Initially, wild type larvae carrying polarity markers were treated with *mex-6* dsRNA. The resulting adults produced embryos that were viable and indistinguishable from wild type embryos. Further improvement of the depletion efficiency confirmed the result, which corresponds to previous described findings (Schubert, Lin et al. 2000).

However, wild type larvae treated with *mex-5* dsRNA grew into adults and produced embryos that were nonviable. For better depletion efficiency I increased the feeding condition from 24 hours to 48 hours and observed three classes of *mex-5*(RNAi) embryos. Class I embryos did not show any polarity establishment defects and divided asymmetrically, as for wild type. Embryos representing class II completely failed to establish polarity, resulting in symmetric cell division.

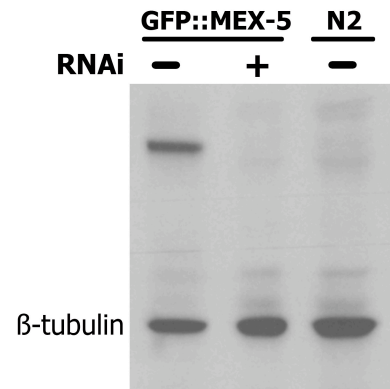
Finally, class III embryos showed the most interesting phenotype. Examination of *mex-5* (RNAi) embryos revealed a delay in polarity establishment, from now on termed partial phenotype. The class III partial phenotype suggests the execution of a correction mechanism during the cell cycle of the embryo, resulting in spindle displacement towards the posterior followed by asymmetric cell division.

The phenotypes were quantified after different feeding conditions. The best possible depletion efficiency was achieved by exposing embryos to *mex-5* dsRNA for approximately 65 hours until the adult stage was reached. Subsequently produced embryos were analyzed by time-lapse microscopy.

Additionally, depletion efficiency was observed by performing western blot analysis of the GFP::MEX-5 fusion protein (Figure 12). GFP::MEX-5 was successfully depleted by dsRNA using the same conditions used for phenotypic analysis.

Figure 12. Western blot analysis of GFP::MEX-5 depletion

The worm strain expressing GFP::MEX-5 fusion protein was treated with *mex-5* dsRNA for 65 hours (RNAi +) or with non-RNAi expressing bacteria as a control (RNAi -). Additionally, N2 wild type worms were treated with non RNAi expressing bacteria. The fusion protein was detected through anti-GFP antibody and β -tubulin functioned as loading control.



Furthermore, time-lapse recordings of *mex-5*(RNAi) embryos were assigned to one of the three classes and the numbers of embryos were compared between worm strains carrying different protein markers (Figure 13).

The majority of mCH::PAR-6; GFP::PAR-2; *mex-5*(RNAi) recorded embryos corresponded class III, the partial phenotype. Less than 10 % were indistinguishable from the wild type. The incidence of class II, the symmetric division phenotype, was limited to only a few embryos. The appearance of class III and class I for worm strains expressing GFP::SPD-2 or GFP::SPD-2; NMY-2::GFP was approximately equal. Hence, over-expression of different protein markers might slightly facilitate or interfere with the mechanism of polarity establishment.

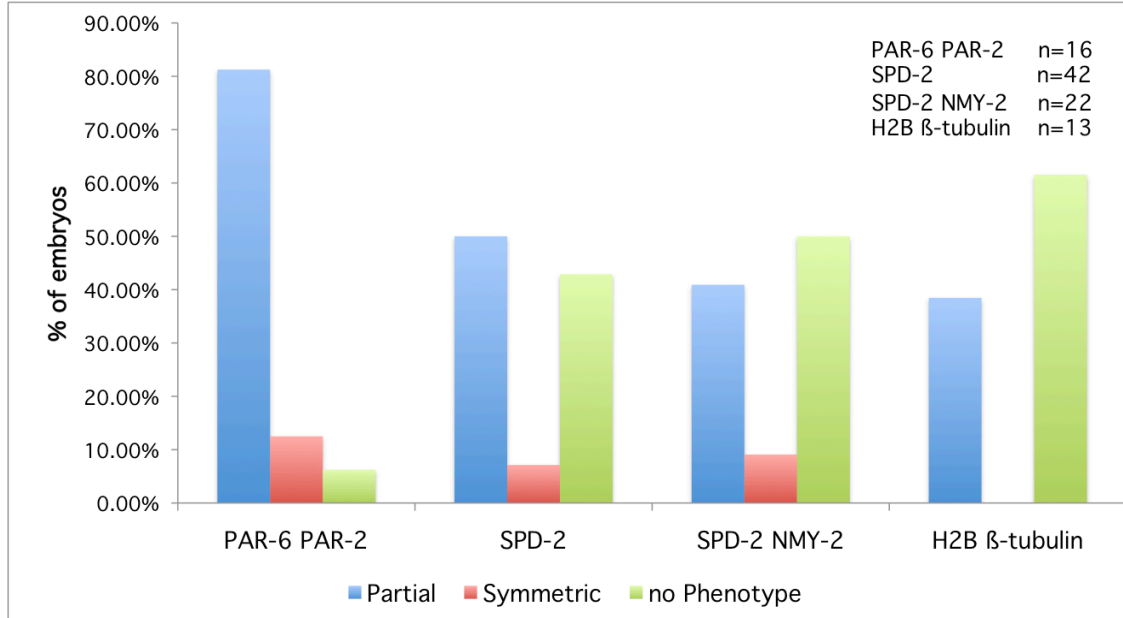


Figure 13. MEX-5 depleted embryos: quantitative phenotypical analysis
Mex-5 (RNAi) embryos of four different worm strains were analyzed and quantified. The number of embryos (in percentage of total embryo number) of each worm strain is shown for three phenotype classes, partial (blue), symmetric (red) and no phenotype (green). [n= total number of embryos]

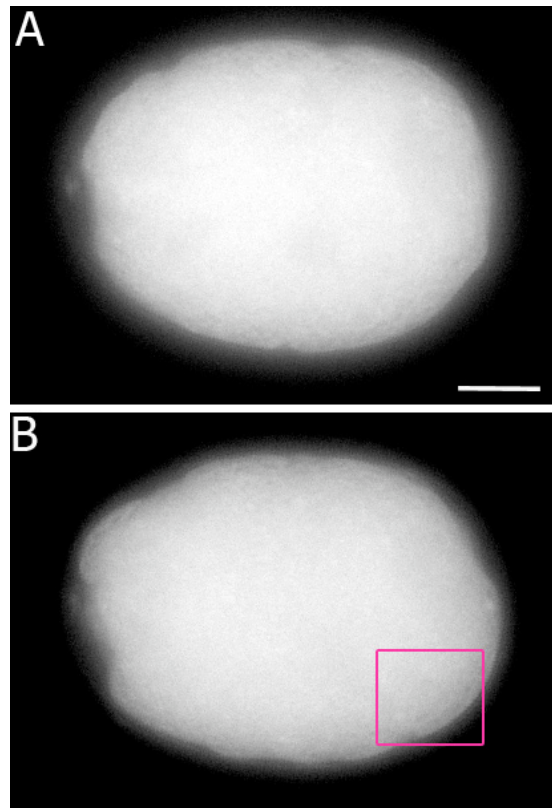
4.2 Localization dynamics of GFP::MEX-5

To observe MEX-5 localization dynamics in embryos, I used a GFP::MEX-5 fusion under the control of the *pie-1* promoter and 3'UTR (Cuenca, Schetter et al. 2003). Time-lapse analysis typically began before polarity was established.

As previously described (Cuenca, Schetter et al. 2003), GFP::MEX-5 shows uniform distribution throughout the cytoplasm at time point of polarity establishment (Figure 14). Additional observations of the centrosome area do not indicate a localized accumulation of GFP::MEX-5 in the one-cell embryo (Figure 14B), whereas MEX-5 localization has been reported at centrosomes at the two-cell stage in the germline blastomere (Schubert, Lin et al. 2000). MEX-5's initial uniform localization might be required for the process of polarity establishment.

Figure 14. GFP::MEX-5 dynamics before polarity establishment

Time-lapse GFP::MEX-5 images of wild type embryos: **[A]** before polarity establishment; **[B]** at polarity initiation; square indicates the male pronucleus region; Bar 10 μm ; posterior to the right and anterior to the left;



After polarity was established (Figure 15), GFP::MEX-5 started to increase in the embryo anterior and the maximal asymmetry was reached by pseudocleavage (Figure 15B). Accumulation on P granules was observed in germline blastomeres.

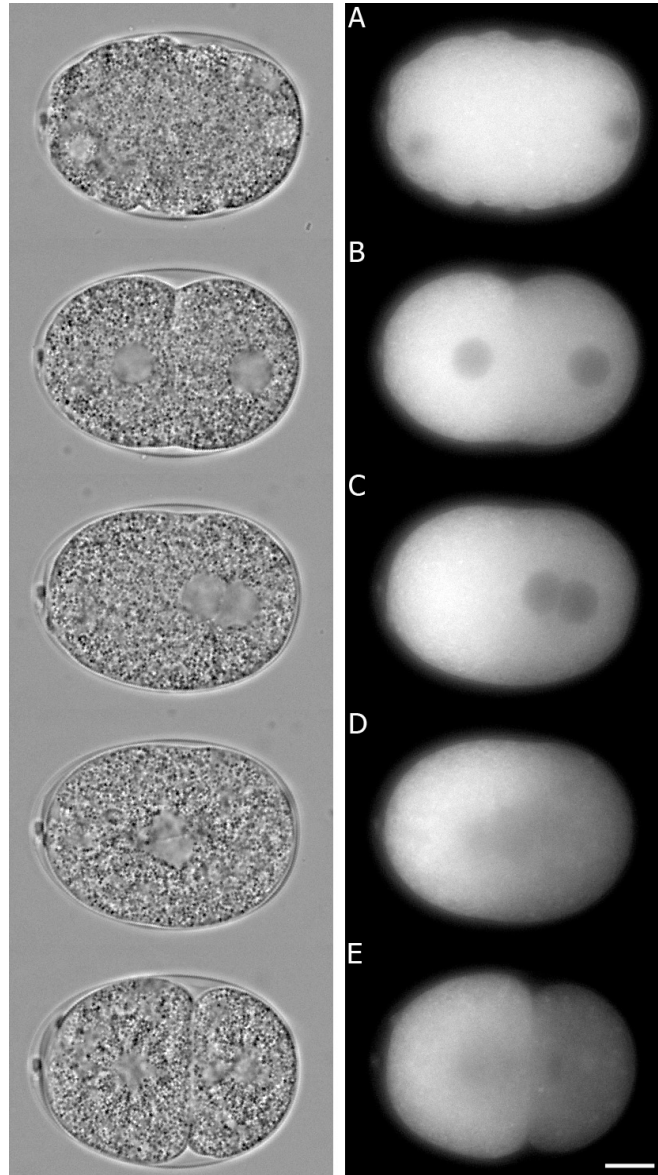


Figure 15. GFP::MEX-5 dynamics in wt embryos

Time-lapse GFP::MEX-5 images to the right and brightfield images to the left. Embryo stages: [A] Pronuclei migration; [B] Pseudocleavage; [C] Pronuclei meeting; [D] Nuclear envelope breakdown; [E] Two-cell stage; Bar 10 μm ; posterior to the right and anterior to the left;

4.3 MEX-5 depleted embryos fail to extend the cortical PAR-2 domain

The establishment of the posterior and anterior polarity domains coincides with the cortical localization of PAR proteins. To determine whether MEX-5 is required for polarity establishment, I examined the dynamics of mCH::PAR-6 and GFP::PAR-2 localization in *mex-5*(RNAi) embryos.

Time-lapse microscopy was performed to observe GFP::PAR-2 and mCH::PAR-6 in embryos depleted of MEX-5 by RNAi (Figure 17). In wild type embryos, the GFP::PAR-2 domain expands simultaneously with the cortical smooth domain and reaches its maximal domain size by pseudocleavage (Cuenca, Schetter et al. 2003) (Figure 17A). In contrast, in 13 out of 16 *mex-5*(RNAi) embryos maintained uniform mCH::PAR-6 (Figure 17 C1-2) until the GFP::PAR-2 domain started to expand at time point of pronuclear meeting, termed partial phenotype (Figure 17 C3-4). The GFP::PAR-2 domain size varied from 10 % to approximately 30 % of embryo length (Figure 16), whereas for wild type embryos domain expansion was observed from 40 to 45 % of embryo length at pronuclear meeting (Figure 17A3). Furthermore, the initial site of GFP::PAR-2 enrichment on the cortex correlated with the site where the male pronucleus formed (Figure 17C1 C4).

The small PAR-2 domain in *mex-5*(RNAi) embryos expanded as the cell cycle proceeded, but only 2 out of 7 *mex-5* embryos reached the wild type domain size of about 45 % of embryo length during cell division (Figure 16). *Mex-5*(RNAi) embryos with partial phenotypes were still able to accomplish asymmetric cell division (Figure 17C6) but the resulting germline blastomeres showed deviations in cell size from the wild type situation. Additionally, the mCH::PAR-6 domain was no longer exclusively restricted to the anterior blastomere. Furthermore, 2 out of 16 *mex-5*(RNAi) embryos failed to establish polarity and divided symmetrically (Figure 17 B6).

The GFP::PAR-2 domain was not visible on the cortex and the protein remained cytoplasmic, whereas mCH::PAR-6 was uniformly localized at the cortex throughout cell division. The results demonstrate that the majority of *mex-5(RNAi)* embryos initially fail to expand the GFP::PAR-2 domain at the cortex. Furthermore, a few MEX-5 depleted embryos completely failed to localize GFP::PAR-2 on the cortex and divided symmetrically.

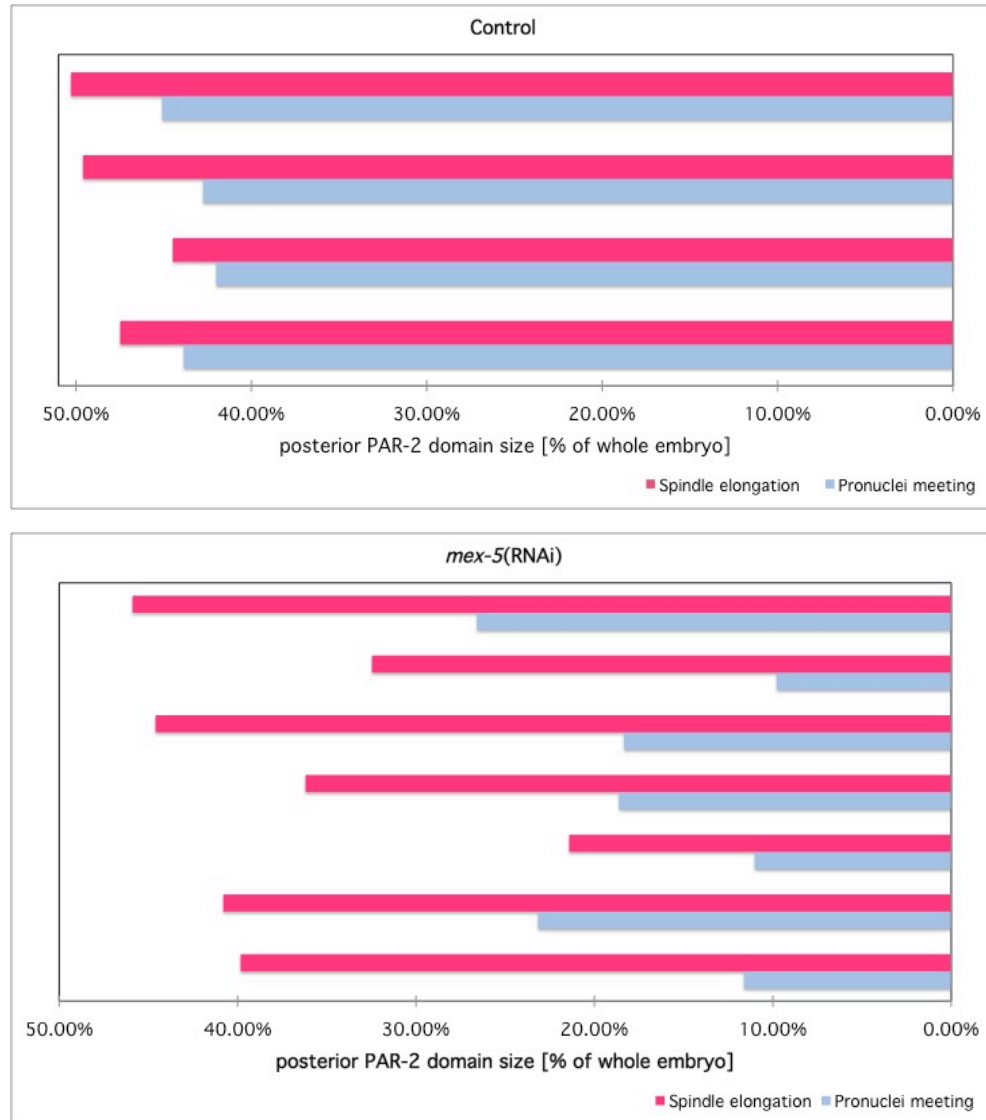


Figure 16. Posterior domain size in wild type embryos and *mex-5(RNAi)* embryos

GFP::PAR-2 domain size was quantified in control and *mex-5(RNAi)* embryos. The domain size was measured at two time points: pronuclear meeting (blue) and spindle elongation (red) and standardized to the whole embryo size.

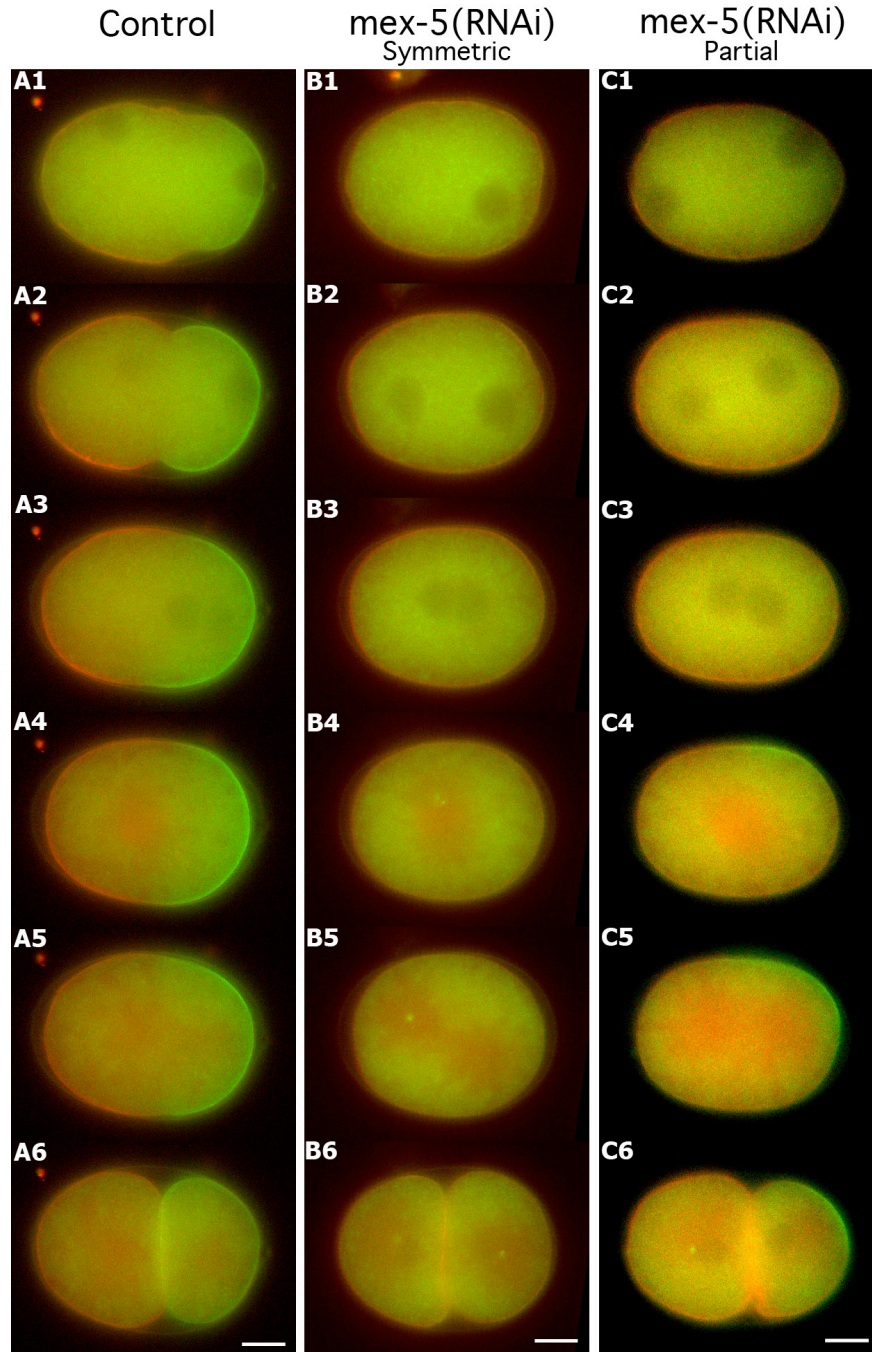


Figure 17. GFP:PAR-2 (green) and mCH::PAR-6 (red) dynamics in *mex-5(RNAi)* embryos

Embryos during [1] pronuclear formation; [2] pronuclear migration and formation of pseudocleavage furrow [A2]; [3] embryos during pronuclear meeting and nuclear envelope breakdown [4]; [5] spindle elongation and two-cell stage embryos [6]; GFP::PAR-2 appears on the cortex around pronuclear meeting but fails to expand [C3-C6]. mCH::PAR-6 remains uniformly distributed throughout the cortex [B], the cell divides symmetrically [B6]. Bars, 10 μ m; posterior to the right and anterior to the left;

4.4 MEX-5 depletion affects the early phase of polarity establishment

The observed localization dynamics of GFP::PAR-2 and mCH::PAR-6 in *mex-5(RNAi)* embryos suggest an involvement of MEX-5 in polarity establishment. For that reason, *mex-5(RNAi)* embryos were further examined to observe phenotypic abnormalities restricted to a specific developmental phase of the embryo. Previous reports suggest that polarity initiation coincides with centrosome-cortex proximity (Cowan and Hyman 2004a).

Therefore, to assess the role of MEX-5 in polarity establishment, centrosomal migration was observed in *mex-5(RNAi)* embryos with the use of the centrosome marker GFP::SPD-2 (Figure 18). Time-lapse recordings were initiated approximately 300 sec before polarity was established. Assembly of the pericentriolar material was quantified by measuring fluorescence intensities.

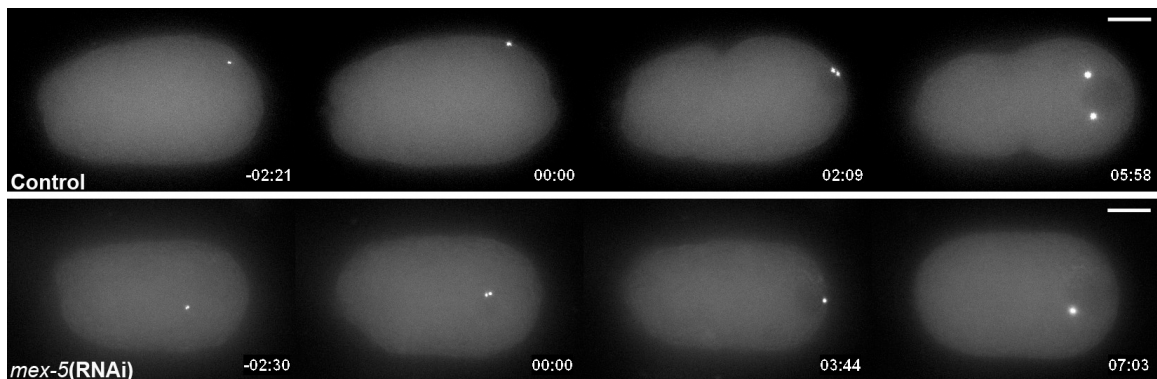


Figure 18. GFP::SPD-2 dynamics in *mex-5(RNAi)* embryos

The GFP::SPD-2 labeled centrosome is visible as a bright dot. In the control images the centrosome lies adjacent to the cortex at the time of polarity initiation (time: 00:00). *Mex-5(RNAi)* embryos at time point 00:00 show approximately the same cell cycle stage but the centrosome is not close to the cortex. Bars, 10 μ m; posterior to the right and anterior to the left; the second centrosome is out of the focal plane in *mex-5(RNAi)* at time point 3:44 and 7:03; mm:ss;

In wild type embryos, after completing two meiotic divisions, the sperm supplied centrosome migrates toward the posterior cortex at time point of polarity establishment. Centrosome-cortex proximity correlates with the initiation of polarity and the cell starts to establish cortical domains.

In contrast, 8 out of 20 *mex-5*(RNAi) embryos showed aberrant centrosome-cortex proximity (Figure 18). The shortest possible distance from the centrosome to the cortex was measured and compared to the cell cycle stage of control embryos. The cell cycle stage was determined by the estimated size of the male pronucleus at time point of polarity initiation.

Shortly before polarity was initiated, wild type centrosomes moved to the cortex and remained at the cortex until the male pronucleus started to migrate. However, centrosomes in *mex-5*(RNAi) embryos showed greater distance to the cortex at time point relative to control polarity establishment (Figure 19).

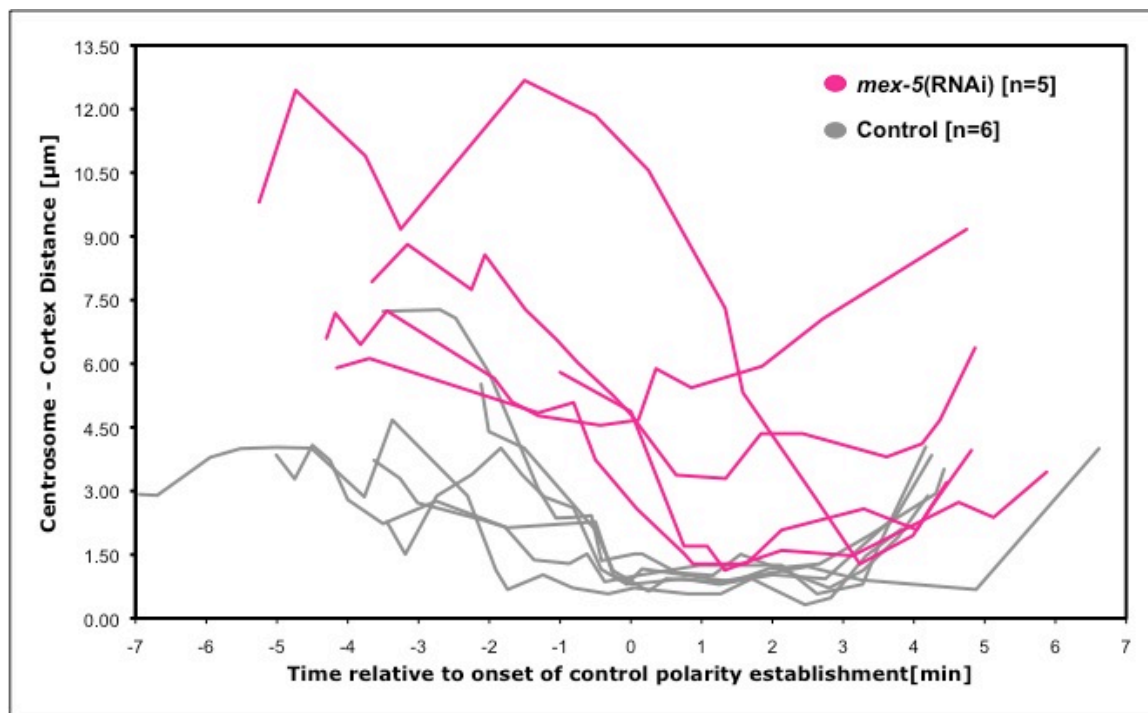


Figure 19. Centrosome-cortex distances during polarity establishment of *mex-5*(RNAi) embryos

Each line represents an embryo and indicates the distance from the centrosome to the nearest point on the cortex over time. Time point was assigned at similar cell cycle stage to that in control embryos at polarity establishment.

At later cell cycle stages, centrosome movement toward the cortex was observed for 3 out of 5 *mex-5(RNAi)* embryos and polarity was established shortly afterwards. Furthermore, 2 out of 5 *mex-5(RNAi)* embryos established polarity without centrosome movement to the cortex.

Additionally, I measured GFP::SPD-2 fluorescence intensities to observe the accumulation of pericentriolar material. In wild type embryos, centrosomes were duplicated at time point of polarity establishment. Separation of centrosomes and continuous accumulation of GFP::SPD-2 to the pericentriolar material caused decreased intensities followed by strong increase. *MEX-5* depleted embryos did not show any abnormal pericentriolar material accumulation; intensities reached values within the control range (Figure 20).

The aberrant centrosome-cortex proximity observed in *mex-5(RNAi)* embryos suggests that *MEX-5* is involved in the early phase of polarity establishment.

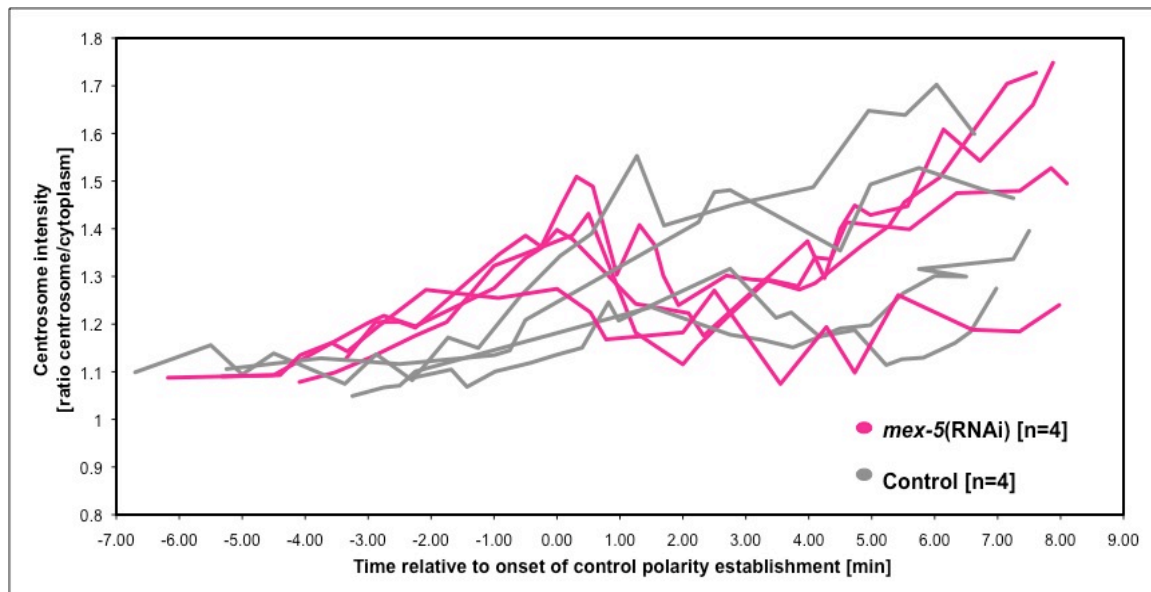


Figure 20. Centrosome maturation of *mex-5(RNAi)* embryos

Centrosome maturation was observed by measuring GFP::SPD-2 intensity levels. Time point was assigned at similar cell cycle stage to that in control embryos at polarity establishment.

4.5 Cortical contractility of *mex-5*(RNAi) embryos is comparable to wild type

Before polarization, the entire embryo cortex undergoes contractions caused by the acto-myosin meshwork. Upon polarization, contractility is locally inhibited at the posterior and expands to half of the embryo. Therefore, polarity establishment requires the modulation of contractility changes caused by changes in the structural basis of the acto-myosin meshwork (Cowan and Hyman 2007).

To assess whether MEX-5 affects the regulation of contractility, I examined GFP::NMY-2; GFP::SPD-2 fluorescence in *mex-5*(RNAi) embryos. The non muscle myosin NMY-2 is a component of the acto-myosin meshwork and the additional centrosome marker protein SPD-2 provided information about polarity establishing defects in *mex-5*(RNAi) embryos.

50 % of the *mex-5*(RNAi) embryos examined were undistinguishable from wild type embryos. Apparently, over-expression of NMY-2 might cause compensation of polarity establishing defects. 9 out of 22 *mex-5*(RNAi) embryos exhibited a partial phenotype, whereas 2 *mex-5*(RNAi) embryos failed to establish polarity and divided symmetrically. To observe polarity establishment, time-lapse recordings were taken approximately 300 sec before polarization. Wild type embryos at polarity initiation show the appearance of the posterior smooth domain and subsequent expansion to the embryo's middle. When expansion of the non-contractile domain reaches the middle of the embryo, the contractile gradient is at its maximum, resulting in the formation of one deep ingression, the pseudo-cleavage furrow.

mex-5(RNAi) embryos representing a partial phenotype were compared to the cell cycle stage at control polarity establishment. The pattern of contractile activity of the cortex in *mex-5*(RNAi) embryos was unchanged.

Prior to polarization, GFP::NMY-2 fluorescence was localized at the entire embryo cortex. Polarity initiation caused the down regulation of contractility at the posterior and the smooth domain expanded to the middle of the embryo.

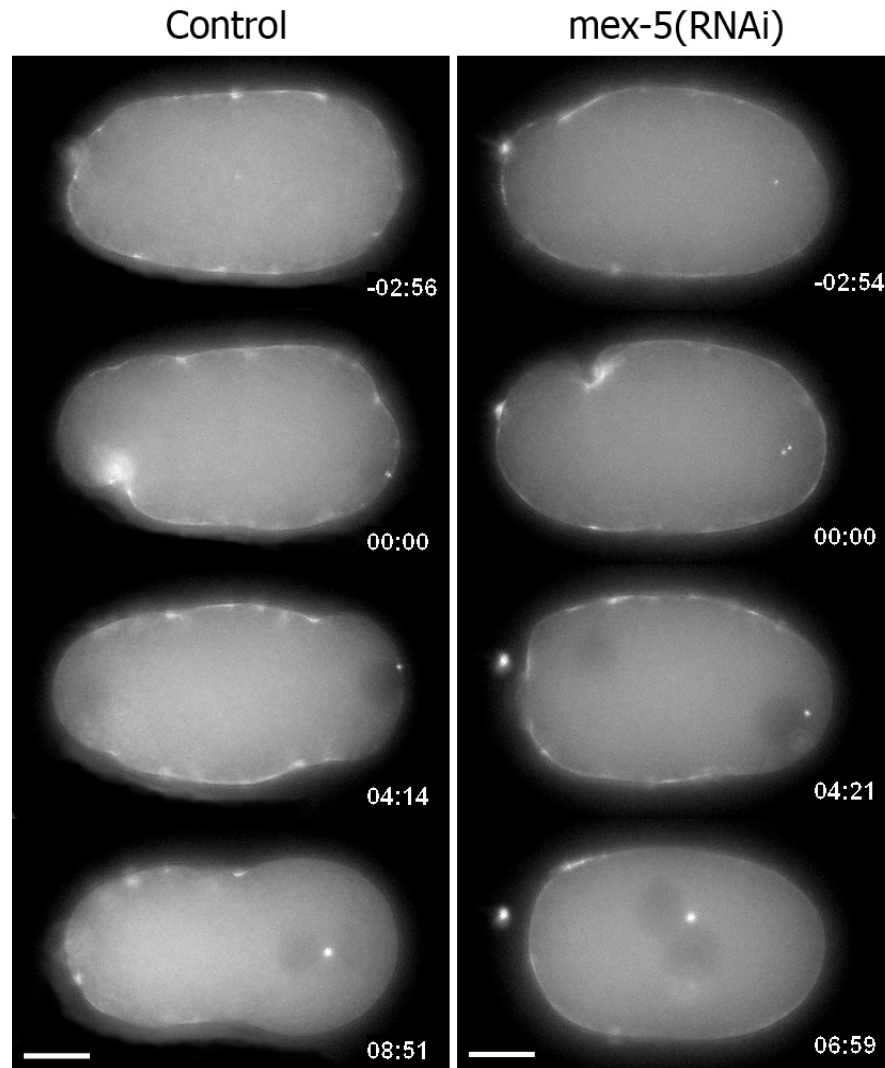


Figure 21. GFP::NMY-2; GFP::SPD-2 dynamics in *mex-5(RNAi)* embryos

Left panel shows images from wild type embryo and the right panel shows the partial phenotype of MEX-5 depleted embryos. GFP::NMY-2 fluorescence indicates dynamic of the acto-myosin cortex, whereas GFP::SPD-2 localizes to the centrosome, visible as a bright dot. Time-point 00:00 represents the cell cycle stage at control polarity establishment. Bars, 10 μ m; posterior to the right and anterior to the left; mm:ss;

Although contractile patterns were unchanged, contractility strength of the cortex in *mex-5(RNAi)* embryos appeared less dominant. Smooth domain boundaries are usually indicated by deeper ingressions, whereas in MEX-5 depleted embryos the distinction is less present. Furthermore, the formation of the pseudocleavage furrow was diminished or completely absent.

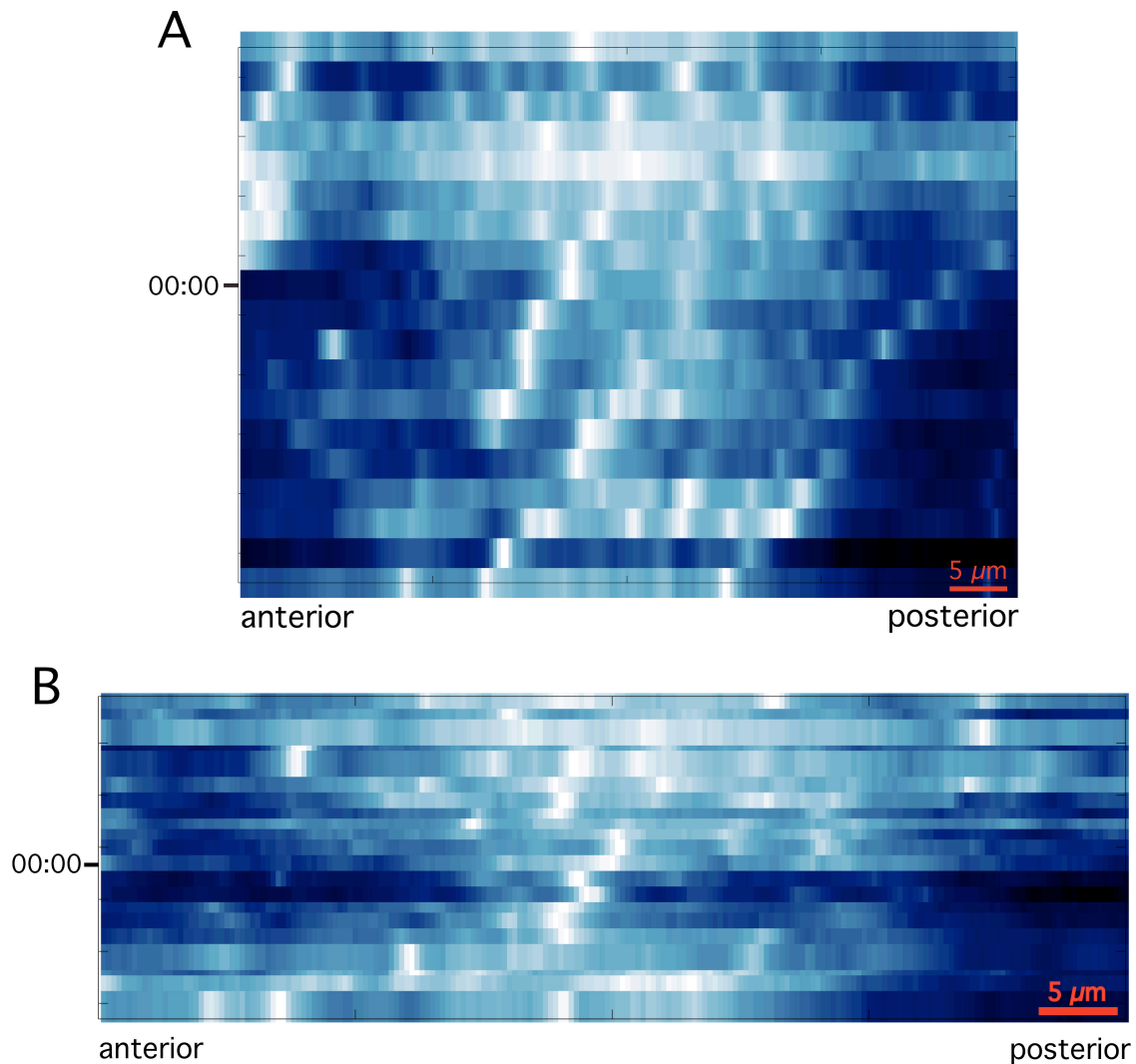


Figure 22. Kymograph: GFP::NMY-2

Intensity values of spatial positions are displayed over time. Intensities were measured from the anterior to the posterior, distance indicated by the bars.

Time point 00:00 was assigned at similar cell cycle stage to that in control embryos at polarity establishment. **[A]** wild type embryo; **[B]** *mex-5(RNAi)* embryo. High intensities appear white and low intensities dark blue.

GFP::NMY-2 intensities were measured at the cortex using a line scan from the anterior to the posterior pole. The intensity values were displayed in a kymograph, giving a two-dimensional graphical representation of spatial position over time. Wild type embryos display the expected intensity pattern, with expanding posterior domain after polarity initiation, represented by dark blue, which indicates diminished NMY-2 intensity. MEX-5 depleted embryos showed comparable intensities pattern. After polarity initiation the contractile domain retracts from the posterior pole to the middle of the embryo.

Therefore, the intensity measurements of GFP::NMY-2 do not indicate an involvement of MEX-5 in the control of the cortex leading to establishment of the non-contractile posterior domain. MEX-5 may have a minor role in modulation of contractile activity.

4.6 Microtubule organization is not affected by MEX-5 depletion

PAR proteins transmit polarity cues from the cortex downstream to mediators of pulling forces, acting along astral microtubules. The downstream signaling generates differential activation of G-proteins and increases net pulling forces at the posterior pole, generating asymmetric spindle position. It has been reported that enrichment of one G protein signaling regulator on the posterior cortex depends on PAR-3 and PAR-2. Embryos defective of G protein signaling regulators show two equal blastomeres, defects in centrosomes, microtubules and spindle positioning in two-cell stage embryos and sometimes chromosome segregation defects (Colombo, Grill et al. 2003).

Therefore, posterior spindle positioning requires correct polarity establishment. Analysis of *mex-5(RNAi)* embryos might indicate a correlation to regulators of microtubule pulling forces. I examined the partial phenotype of *mex-5(RNAi)* embryos in respect of abnormalities in spindle, microtubule and centrosome behavior.

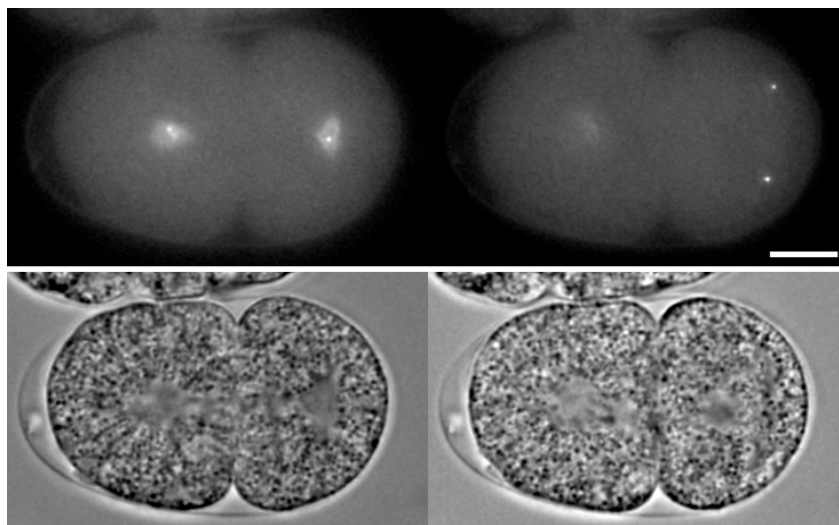


Figure 21. P1 centrosome separation in *mex-5(RNAi)* embryos

Upper images, GFP::SPD-2 time-lapse recording at two-cell stage. Lower row represents brightfield images; Bar 10 μm ; posterior to the right and anterior to the left;

In several recordings using GFP::SPD-2 fluorescence I observed abnormalities in the centrosome attachment to the nucleus. First, at pronuclei migration the male pronucleus started to migrate away from the cortex and one of the duplicated centrosomes detached from the pronucleus and migrated back to the cortex (Figure 22). Furthermore, *mex-5*(RNAi) embryos after cell division showed aberrant dissociation of centrosomes in the P1 germline blastomere (Figure 21). Both observations suggest weak attachment of centrosomes to the pronucleus. Reduced spindle pole rocking during mitosis in *mex-5*(RNAi) embryos was the most prominent observed abnormality regarding spindle positioning. To elucidate microtubule structure and chromosome segregation, I performed time-lapse recordings of GFP::histone 2B and GFP:: β -tubulin (Figure 23). The appearance of the spindle in *mex-5*(RNAi) embryos was comparable to wild type at all cell cycle stages, and chromosome segregation also appeared normal. Hence, my observations suggest that microtubule organization and function are not affected by MEX-5 depletion. However, MEX-5 might influence the centrosome attachment to the nucleus. Localization of GFP::MEX-5 specifically on the germline centrosomes in P1 would suggest a mechanism related to centrosome attachment.

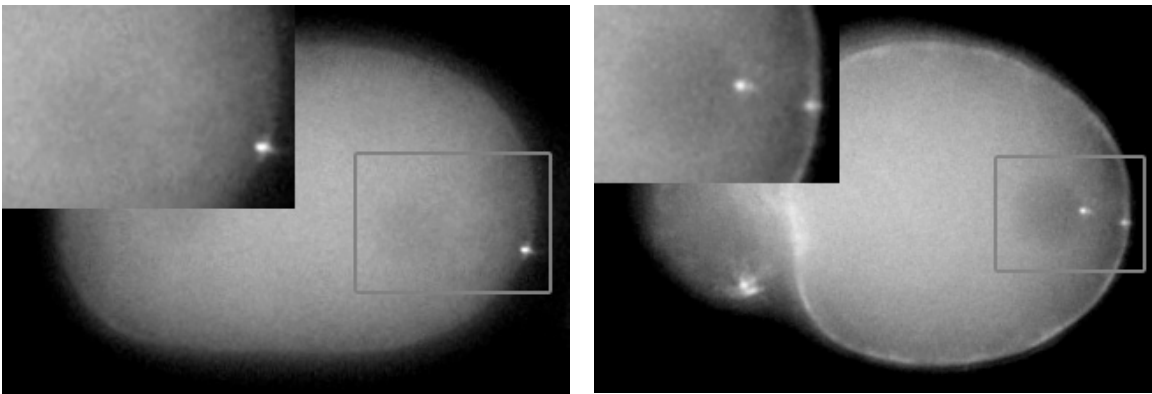


Figure 22. Centrosome detachment from male pronucleus in *mex-5*(RNAi) embryos

Left image: GFP::SPD-2 fluorescence recording, square represents higher magnification of male pronucleus and centrosomes. To the right: GFP::NMY-2; GFP::SPD-2 recording, higher magnification of the male pronucleus and centrosomes. Bar 10 μ m; posterior to the right and anterior to the left;

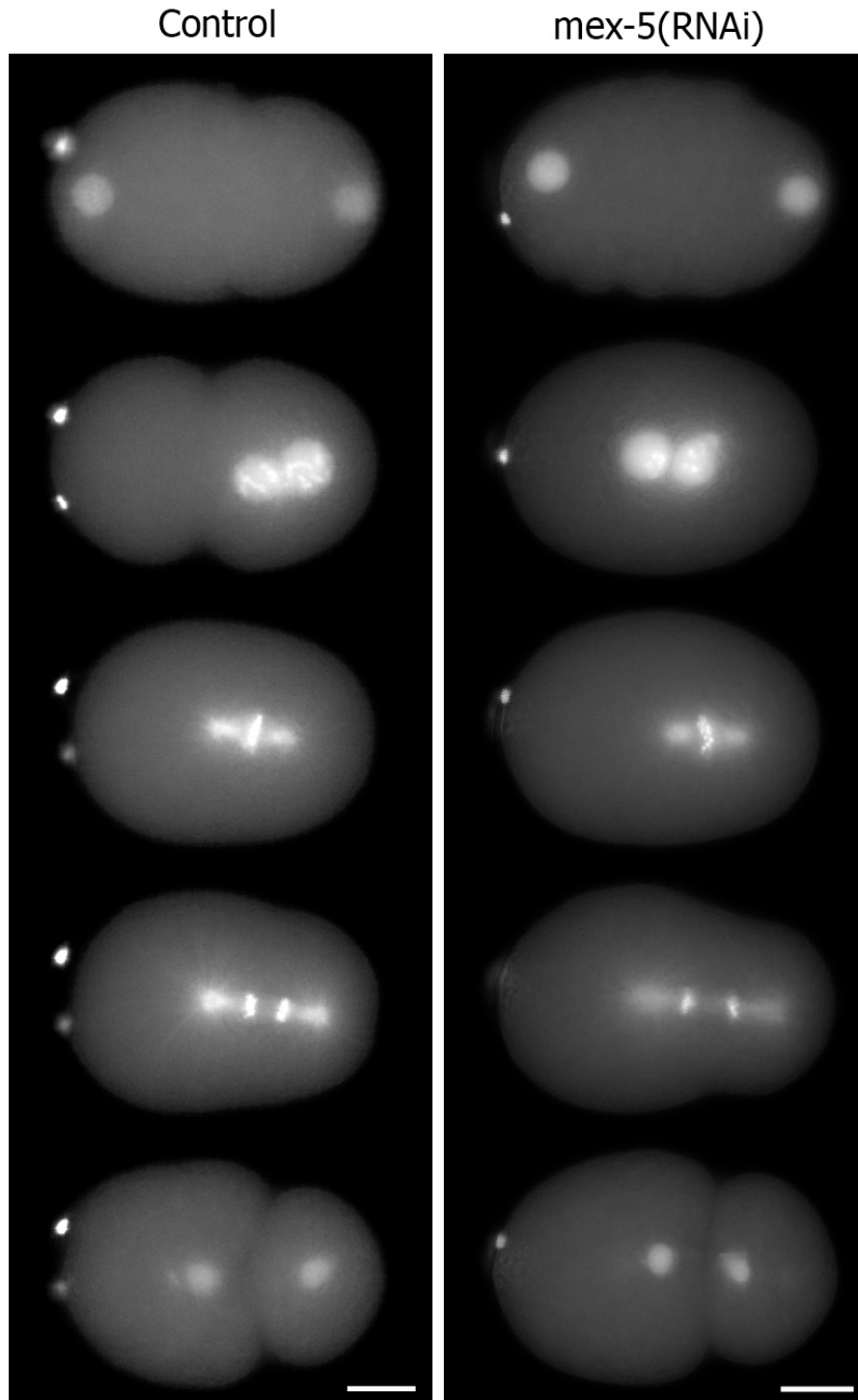


Figure 23. GFP::H2B and GFP:: β -tubulin in control and *mex-5(RNAi)* embryos

Left panel: wild type embryo; right panel: *mex-5(RNAi)* embryo. Top down, embryo stages: Pronuclear migration; Pronuclear meeting; Spindle displacement; Spindle elongation and two-cell stage; Bars, 10 μ m; posterior to the right and anterior to the left;

5 Discussion

To examine the role of MEX-5 and MEX-6 in polarity establishment, I have taken advantage of the potential to combine live-cell imaging techniques with an analysis of dsRNA treated embryos. I investigated the effects of MEX-5 and MEX-6 RNAi-mediated depletion in the *C.elegans* one-cell embryo.

MEX-6 depleted embryos didn't show any phenotypical aberrations from wild type embryos. Thus, embryos from MEX-6 RNAi treated adults grew into fertile adults. These observations are consistent with previous findings (Schubert, Lin et al. 2000) and suggest that *mex-6* is a nonessential gene. However, *mex-5*(RNAi) embryos are nonviable and phenotypic analysis revealed defects in polarity. The most striking polarity defects resulted in symmetric cell division. However the majority of *mex-5*(RNAi) embryos exhibited partial polarity defects and asymmetric cell division. Quantitative analysis of the phenotypes analyzed in worm strains with different marker proteins revealed different penetrance of polarity defects. Overexpression of fluorescently tagged proteins within the embryo might slightly facilitate or impede polarity defects caused by MEX-5 depletion. For instance, the mCH::PAR-6; GFP::PAR-2 worm strain displayed the smallest number of *mex-5*(RNAi) embryos without defects. Hence, the antagonistic effect between PAR-6 and PAR-2 might cause shifting to more severe polarity defects if one of those proteins is affected by MEX-5 depletion. Furthermore, the worm strain carrying GFP::NMY-2; GFP::SPD-2 was less prone to polarity defects. The slight overexpression of the acto-myosin structural component, NMY-2, might help compensate polarity establishment defects caused by depletion of MEX-5.

My results suggest a model in which MEX-5 functions in polarity establishment, affecting PAR protein localization and centrosome-cortex proximity.

Initially, to observe the formation of the polarity domains I examined the dynamics of PAR-6 and PAR-2 in *mex-5(RNAi)* embryos. Interestingly, formation of the PAR-2 posterior domain was affected. PAR-2 displayed delayed localization dynamics to the cortex and failed to expand the posterior domain to its wild type length but still resulted in asymmetric cell division. In contrast to the wild type situation, both PAR-2 and PAR-6 were localized to the germline blastomere after cell division in *mex-5(RNAi)* embryos. My observations would support a model in which initial polarity defects are corrected by an unknown rescue mechanism at the onset of polarity maintenance. However, the PAR-2 domain localization defect suggests functional involvement of MEX-5 in polarity establishment.

To further elucidate the functional role of MEX-5, I observed centrosome movement to the cortex at polarity initiation. It is known that centrosome-cortex proximity correlates with the polarity initiation event (Cowan and Hyman 2004a). In *mex-5(RNAi)* embryos, the centrosome failed to move to the cortex at the normal time of polarity establishment, suggesting that MEX-5 is required for the early event of polarity establishment. Further analysis of the pericentriolar material formation did not show any defects in centrosome maturation.

Additionally, the activity of the acto-myosin cortex was observed to investigate whether MEX-5's activity is required for the formation of contractile polarity. Time-lapse analysis of the acto-myosin marker protein did not show any effect on the overall pattern. I observed that the ingression formation of the pseudocleavage was less dominant than in wild type. However, resulting measurements of cortical intensities did not show significantly decreased values.

Consistent with previous findings (Cuenca, Schetter et al. 2003), MEX-5 depletion affects PAR-2 domain formation and therefore the formation of cortical polarity domains. Additionally, I observed defects in the centrosome-cortex proximity suggesting an involvement of MEX-5 in the early event of polarity establishment.

Additionally, to gain information about signaling defects downstream of PAR polarity, I examined the microtubule appearance in *mex-5(RNAi)* embryos important for asymmetric positioning of the mitotic spindle. Phenotypical analysis revealed spindle rocking defects during mitosis, centrosome detachment from the male pronucleus and defects in the centrosomal separation in P1. Microtubule structure seemed to be unaffected by MEX-5 depletion as well as chromosome segregation. However, microtubule attachment to the cortex and to the pronuclear envelope might be affected. The transmission of pulling forces generated at the plasma membrane might be attenuated resulting in spindle rocking defects. Furthermore, attachment of centrosomes to the pronucleus depends on the pronuclear lamina and interaction of microtubules with dynein (Meyerzon, Gao et al. 2009). However, a molecular connection between MEX-5 and microtubule activity remains elusive.

What is the functional mechanism of MEX-5 affecting polarity establishment? MEX-5's protein structure might provide the answer to elucidate the functional mechanism. Recent findings suggest that MEX-5's tandem zinc finger domains are involved in binding specific sequences in 3'UTR of mRNAs (Pagano, Farley et al. 2007). Influencing the translational activity of mRNAs is a potential mechanism to specifically regulate and localize protein activity to its target function. One indication for this model might be the uniform distribution of MEX-5 during polarity establishment. MEX-5 would specifically destabilize mRNA to inhibit protein function during polarity establishment. Investigations of MEX-5's zinc finger domains have shown that the structural basis do not provide enough mRNA binding specificity (Pagano, Farley et al. 2007). Proteins like PLK-1 and PLK-2 may function to provide binding specificity through phosphorylation activity. However to elucidate the polarity establishment defect prior MEX-5 depletion, RNA and protein binding activity needs to be further investigated.

6 References

- Abrash, E. and D. Bergmann (2009). "Asymmetric Cell Division: A View from Plant Development." *Development Cell* **16**: 783-796.
- Albertson, D. (1984). "Formation of the first cleavage spindle in nematode embryos." *Dev. Biol.* **101**: 61-72.
- Asaoka-Taguchi, M., M. Yamada, et al. (1999). "Maternal Pumilio acts together with Nanos in germline development in *Drosophila* embryos." *Nature Cell Biology* **1**: 431-437.
- Brenner, S. (2009). "In the Beginning was the Worm." *Genetics* **182**(413-415).
- Cheeks, R., J. Canman, et al. (2004). "C. elegans PAR proteins function by mobilizing and stabilizing asymmetrically localized protein complexes." *Current Biology* **14**: 851-862.
- Cheng, N., C. Kirby, et al. (1995). "Control of cleavage spindle orientation in *Caenorhabditis elegans*: the role of the genes PAR-2 and PAR-3." *Genetics* **139**: 549-559.
- Colombo, K., S. Grill, et al. (2003). "Translation of Polarity Cues into Asymmetric Spindle Positioning in *Caenorhabditis elegans* Embryos." *Science* **300**: 1957-1961.
- Cowan, C. and A. Hyman (2004a). "Centrosomes direct cell polarity independently of microtubule assembly in *C. elegans* embryos." *Nature* **431**: 92-95.
- Cowan, C. and A. Hyman (2004b). "Asymmetric Cell Division in *C. elegans*." *Annu. Rev. Cell Dev. Biol.* **20**: 427-53.
- Cowan, C. and A. Hyman (2007). "Actomyosin reorganization and PAR polarity in *C. elegans*." *Development* **134**: 1035-1043.
- Cuenca, A., A. Schetter, et al. (2003). "Polarization of the *C. elegans* zygote proceeds via distinct establishment and maintenance phases." *Development* **130**(7): 1255-1265.
- DeRenzo, C., K. Reese, et al. (2003). "Exclusion of germ plasm proteins from somatic lineages by cullin-dependent degradation." *Nature* **424**: 685-689.
- Drubin, D. and W. Nelson (1996). "Origins of Cell Polarity." *Cell* **84**: 335-344.
- Evans, T., S. Crittenden, et al. (1994). "Translational control of maternal glp-1 mRNA establishes an asymmetry in the *C. elegans* embryo." *Cell* **77**(2): 183-94.
- Glotzer, M. (2005). "The molecular requirements for cytokinesis." *Science* **307**: 1735-1739.
- Goenczy, P. and L. Rose (2005). "Asymmetric cell division and axis formation in the embryo." *WormBook*, ed. The *C. elegans* Research Community.
- Grill, S., P. Gönczy, et al. (2001). "Polarity controls forces governing asymmetric spindle positioning in the *Caenorhabditis elegans* embryo." *Nature* **409**: 630-633.
- Guedes, S. and J. Priess (1997). "The *C. elegans* MEX-1 protein is present in germline blastomeres and is a P granule component." *Development* **124**(4): 731-9.
- Guedes, S. and J. Priess (1997). "The *C. elegans* MEX-1 protein is present in germline blastomeres and is a P granule component." *Development* **124**: 731-739.
- Hird, S. and J. White (1993). "Cortical and Cytoplasmic Flow Polarity in Early Embryonic Cells of *Caenorhabditis elegans*." *The Journal of Cell Biology* **121**: 1343-1355.
- Hodgkin, J. (2005). "Introduction to genetics and genomics." *WormBook*, ed. The *C. elegans* Research Community.

- Hyman, A. and J. White (1987). "Determination of cell division axes in the early embryogenesis of *Caenorhabditis elegans*." *J. Cell Biol.* **105**: 2123-35.
- Jenkins, N., J. Saam, et al. (2006). "CYK-4/GAP provides a localized cue to initiate anteroposterior polarity upon fertilization." *Science* **313**: 1298-1301.
- Kemphues, K. (2000). "PARsing Embryonic Polarity." *Cell* **101**: 345-348.
- Knoblich, J. (2008). "Mechanisms of Asymmetric Stem Cell Division." *Cell* **132**: 583-597.
- Mello, C., B. Draper, et al. (1992). "The PIE-1 and MEX-1 genes and maternal control of blastomere identity in early *C. elegans* embryos." *Cell* **70**: 163-176.
- Mello, C., C. Schubert, et al. (1996). "The PIE-1 protein and germline specification in *C. elegans* embryos." *Nature* **382**: 710-712.
- Meyerzon, M., Z. Gao, et al. (2009). "Centrosome attachment to the *C. elegans* male pronucleus is dependent on the surface of the nuclear envelope." *Developmental Biology* **327**: 433-446.
- Motegi, F. and A. Sugimoto (2006). "Sequential functioning of the ECT-2 Rho-GEF, RHO-1 and CDC-42 establishes cell polarity in *Caenorhabditis elegans* embryos." *Nature Cell Biology* **8**: 978-985.
- Munro, E. (2006). "PAR proteins and the cytoskeleton: a marriage of equals." *Current Opinion in Cell Biology* **18**: 86-94.
- Munro, E., J. Nance, et al. (2004). "Cortical Flows Powered by Asymmetrical Contraction Transport PAR Proteins to Establish and Maintain Anterior-Posterior Polarity in the Early *C. elegans* Embryo." *Developmental Cell* **7**: 413-424.
- Neumueller, R. and J. Knoblich (2009). "Wicked views on stem cell news." *Nature Cell Biology* **11**(6): 678-9.
- Nishi, Y., E. Rogers, et al. (2008). "Polo kinases regulate *C. elegans* embryonic polarity via binding to DYRK2-primed MEX-5 and MEX-6." *Development* **135**: 687-697.
- Pagano, J., B. Farley, et al. (2007). "Molecular Basis of RNA recognition by the embryonic Polarity determinant MEX-5." *The Journal of Biological Chemistry* **282**: 8883-8894.
- Rolls, M. and C. Doe (2003). "From embryo to axon." *Nature* **421**: 905-906.
- Schonegg, S. and A. Hyman (2006). "CDC-42 and RHO-1 coordinate acto-myosin contractility and PAR protein localization during polarity establishment in *C. elegans* embryos." *Development* **133**: 3507-3516.
- Schubert, C., R. Lin, et al. (2000). "MEX-5 and MEX-6 function to establish Soma/Germline asymmetry in early *C. elegans* Embryos." *Molecular Cell* **5**: 671-682.
- Seydoux, G. and A. Fire (1994). "Soma-germline asymmetry in the distributions of embryonic RNAs in *Caenorhabditis elegans*." *Development* **120**(10): 2823-34.
- Tabara, H., R. Hill, et al. (1999). "POS-1 encodes a cytoplasmic zinc finger protein essential for germline specification in *C. elegans*." *Development* **126**: 1-11.
- Varnum, B., Q. Ma, et al. (1991). "The TIS11 primary response gene is a member of a gene family that encodes proteins with a highly conserved sequence containing an unusual Cys-His repeat." *Mol Cell Biology* **11**(3): 1754-8.

7 Appendix

7.1 Abbreviations

MEX	muscle excess	C. elegans	Caenorhabditis elegans
GEF	guanidine exchange factor	D. melanog.	Drosophila melanogaster
GTP	guanidine triphosphate	CYK	cytokinesis
UTR	untranslated region	GAP	GTPase activating protein
PAR	partitioning defective	aPKC	atypical protein kinase C
POS	posterior segregation	ECL	enhanced chemiluminescence
SKN	skinhead	PIE	pharynx and intestine in excess
mRNA	messenger RNA	RNA	ribonucleic acid
DNA	deoxyribonucleic acid	ZIF	zinc finger interacting protein
TTP	tristetraprolin	IPTG	Isopropyl thiogalactopyranosid
NMY	non muscle myosin	SPD	spindle defective
H2B	histone 2B	NGM	nematode growth medium
PLK	Polo kinase	FBS	fetal bovine serum
PBS	phosphate buffered saline	LB	Luria Bertani
SDS	Sodium dodecyl sulfate	Amp	Ampicillin
Tet	Tetracycline	HRP	horse radish peroxidase
dsRNA	doublestrand RNA	wt	wild type

7.2 Curriculum vitae

Personal information

First name / Surname	Silke REITER
Address	Hermannngasse 2a/121, 1070 Vienna
E-mail	silke.reiter1@gmx.net
Date of Birth	30.07.1984
Nationality	Austrian

Education

High-school	Handelsakademie Steyr	1998-2003
Subject of study	Molecular Biology	2003-2009
Name of University	University of Vienna, Austria	

Research experience

Date	October 2008 – December 2009
Research Group	Carrie R. Cowan, IMP - Institute of Molecular Pathology
Diploma Thesis	The cytoplasmic cell fate regulator Mex-5 is required for the establishment of cortical polarity in the C.elegans one-cell embryo

Date	July, August 2006
Research Group	Wiche G., Max F. Perutz Laboratories, Vienna
Project	FRET analysis of interactions between the cytolinker Plectin and Alpha Actinin

Date	April, May 2008
Research Group	Skern T., Max F. Perutz Laboratories, Vienna
Project	Investigation of the NS2B-3 proteinase cleavage properties of TBEV

Work experience

Date	January 2007 – January 2008
Research Group	Juergen Knoblich, IMBA, Vienna
Position	Research Technician

Poster presentation

Date	June 2009
Title	The cytoplasmic cell fate regulator MEX-5 is required for the establishment of cortical polarity
Place	“International Worm Meeting”, Los Angeles

Languages

Mother tongue	German
Other languages	English (fluent), Spanish (Basic user)